

Journal of Advances in Engineering and Technology

Editor-in-Chief:

Prof. Dr. José Pereira

Universidade de Lisboa, Portugal

Copyright © 2025. ASIA PACIFIC SCIENCE PUBLICATIONS
COMPANY LIMITED. Complimentary Copy.

Journal of Advances in Engineering and Technology

Journal of Advances in Engineering and Technology (JAET) is an international, peer-reviewed and open access journal which publishes original articles, reviews, short communications, case studies and letters in the field of electronic research and application. It covers mainly but not limits to the following areas:

- Civil Engineering
- Mechanical Engineering
- Electrical Engineering
- Chemical Engineering
- Aerospace Engineering
- Computer Science and Engineering
- Environmental Engineering
- Materials Science and Engineering
- Biomedical Engineering
- Energy Engineering
- Robotics and Automation

About Publisher:

Asia Pacific Science Press (APSP) is a swiftly expanding publisher of peer-reviewed and open-access journals, strategically located in Hong Kong. As a reliable and esteemed corporation, APSP is dedicated to promoting and serving a wide array of subject areas, ultimately contributing to the betterment of humanity. By disseminating knowledge to a global community of scholars, practitioners, researchers, and students, we strive to establish ourselves as the world's leading independent academic and professional publisher.

Submission instructions: You can submit your manuscript through the official website (www.apspublisher.com) or email (editor.jaet@apspublisher.com), All manuscripts will go through a rapid peer review and production, making the process of publishing simpler and more efficient.

Publisher Headquarter

Room 03, 7th Floor, Block B, Tuen Mun Industrial Centre, 2 New Ping Street, Tuen Mun, Hong Kong, China
Website : www.apspublisher.com
Email : info@apspublisher.com

Fujian Province Office, China

603-1, 6th Floor, Building B20, Chengyi North Street, Software Park, Jimei District, Xiamen City, Fujian Province, China
Website : <https://ojs.apspublisher.com/index.php/amit>
Email : amit@apspublisher.com

Table of Contents

- 1 Differential Dynamics Modeling and Simulation Analysis of Multi-Agent Cooperative Motion**
Shao Qiang
- 8 The Nonlinear Mathematical Modeling and Optimization of Distributed Control in Complex Systems**
Shao Qiang
- 16 A literature Review of Ant Colony Algorithm Based on Cite Space**
Shiyu Li , Shengpan Yang, Jie Jin
- 25 Analysis on Intrinsic Vibration Characteristics of Disc-Lobe Coupling System of Marine gas Turbine**
Zhuoying Li
- 31 Design and Application of a High-Dimensional Robust Control Chart for Joint Monitoring of Location and Scale Parameters**
Meiling Lu
- 40 Graph-Based Deep Learning for E-Commerce Fraud Detection**
Ricardo Mendonça, Antonio Salazar, Elena Martinez
- 50 Optimizing Cybersecurity Incident Response via Adaptive Reinforcement Learning**
Tobias Klein, Giovanni Romano

Differential Dynamics Modeling and Simulation Analysis of Multi-Agent Cooperative Motion

Shao Qiang*

Gaston Day School Shanghai Shangde, Shanghai 201315, China

*Corresponding author: Shao Qiang , sost12822@163.com

Copyright: 2025 Author(s). This is an open-access article distributed under the terms of the Creative Commons Attribution License (CC BY-NC 4.0), permitting distribution and reproduction in any medium, provided the original author and source are credited, and explicitly prohibiting its use for commercial purposes.

Abstract: With the widespread application of multi-agent systems (MASs) in fields such as drone formations, autonomous driving, and robotic swarms, achieving efficient collaboration and stable motion among agents has become a key research focus. This study begins by describing the vertices of agents relative to the formation centroid to enable collision avoidance and formation shape tracking control. Using the Lyapunov direct method, a heat-equation-based collective dynamics model for multi-agent systems is established, providing stability criteria for the model and a leader-follower algorithm. The model enables the transformation from continuous multi-agent systems to discrete systems, completing the cooperative motion of real multi-agent systems. Simulation analysis verifies the effectiveness of the proposed model and control strategy. In a typical simulation scenario, follower agents achieve consensus with leader agents within approximately 10 seconds, with the number of path nodes reduced to just six, zero obstacle collisions, and a computation time of only 49.6 seconds. The proposed control method significantly enhances the cooperative efficiency and motion stability of multi-agent systems under limited information exchange and complex environmental conditions, offering robust theoretical support for the collaborative control of future intelligent systems.

Keywords: Multi-agent Systems; Cooperative Motion; Differential Dynamics Model; Model Stability; Follower Algorithm

Published: Jan 14, 2025

DOI: <https://doi.org/10.62177/jaet.v2i1.151>

1. Introduction

In recent years, multi-agent systems (MASs) have been widely applied in various fields such as drone formations, autonomous driving, and robotic swarms^[1]. Compared to single-agent systems, MASs are more efficient and reliable in task execution and can accomplish complex and challenging tasks that are difficult or even impossible for single-agent systems^[2]. When multiple agents perform tasks, they typically achieve the overall objective optimally through local information sharing and mutual cooperation^[3-4]. Research on the cooperative motion of multi-agent systems provides the necessary theoretical foundation for the organization and autonomous coordination control of complex MASs, while also having a profound impact on practical applications such as intelligent transportation, robotic swarms, and environmental monitoring.

However, in the control of cooperative motion for MASs, designing an efficient and robust control strategy that enables agents to collaborate effectively in dynamic environments remains a challenging problem. In particular, complex real-world scenarios introduce challenges such as interactions between agents, sensor errors, and environmental disturbances, making the control of MASs more intricate. Therefore, optimizing the cooperative motion of MASs while ensuring system stability has become a key issue in current research. The differential dynamics model, as an important continuous-time control framework,

effectively describes the motion behavior of MASs and their interactions. Unlike traditional discrete control methods, the differential dynamics model transforms the agents' motion and control strategies into differential equations, allowing a more precise mathematical representation of their dynamic behavior. This model enables the design of cooperative control strategies suitable for complex environments, ensuring collaboration and motion consistency among agents in dynamic scenarios.

This study builds on the foundation of formation control and system behavior control for MASs, constructing a distributed differential dynamics model for cooperative motion control using the Lyapunov method. Based on this model, control strategies adaptable to different scenarios are designed, and the effectiveness of the proposed model and control strategies is validated through simulation analysis.

2. Cooperative Motion Formation Path Planning for Multi-Agent Systems

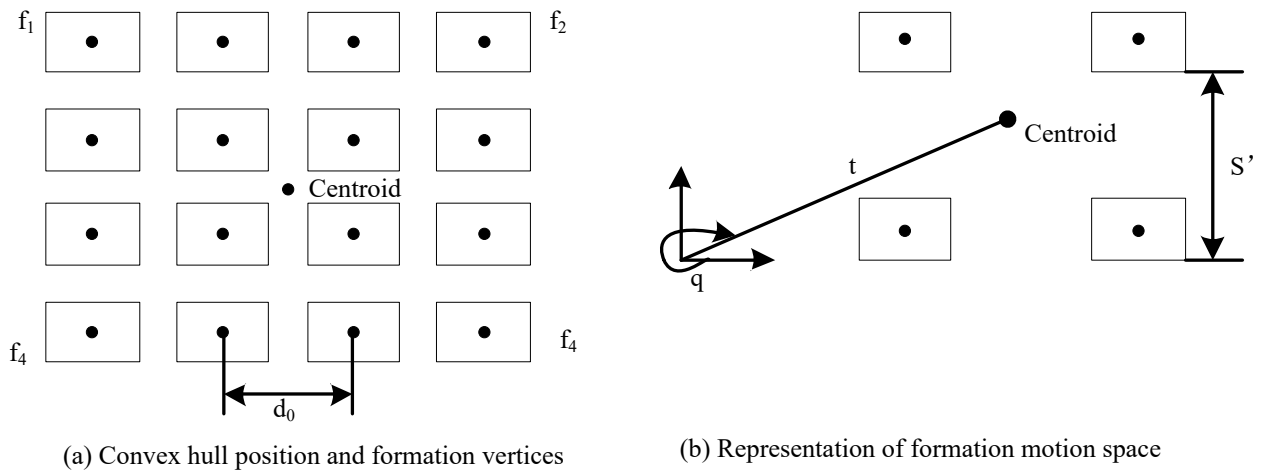
2.1 Formation Control of the Group

The control of group formation behavior is to achieve collision-free movement in multi-agent formation tasks while maintaining a specific formation shape^[5]. First, multiple agents are organized into a square shape for movement. The model is based on a square formation structure f composed of multiple agents. The definition of the cooperative motion formation is shown in Figure 1. In this structure, a set $\{f_1^i, f_2^i, \dots, f_n^i\}$ is used to describe the specific position of the agent in the formation shape. In this paper, the position is the four corners of the four vertices of the square. A distance parameter d is introduced to represent the distance between any two agents in the formation. d allows the agents to maintain a certain distance in the group formation, thereby achieving the stability of the group formation.

The kinematics of each agent are assumed to be the same, and $\{p_1^i, p_2^i, \dots, p_n^i\}$ is used to represent their positions. The outer contour of the formation is represented by the intersection points formed by the positions of the agents in the formation. The smallest convex polygon that surrounds all agents at the intersection points directly displays the overall shape and size of the formation. The formation model can be constructed by combining the formation positions of the agents with the relative vertices. The formation optimization variables can be determined by $x = (t, s'q)$. The variables in this paper include the relative positions of the agents, directional accelerations, and the cumulative deviations between the agents and the target states. The positions of the agents and the vertices of the formation are represented by the above variables as follows:

$$\begin{aligned} p_j^i &= t + s' \text{rot}(q, p_j^i) \quad \forall j \in [1, n] \\ f_j^i &= t + s' \text{rot}(q, f_j^i) \quad \forall j \in [1, n_i] \end{aligned} \quad (1)$$

Figure 1 Definition of coordinated movement formation



All these position and orientation data combined form the configuration of motion at a given moment, representing the set of all possible positions and orientations. In a multi-agent system, each agent controls its respective position and orientation to ensure the entire formation remains consistently stable.

2.2 Behavior Control of Intelligent Group Systems

To prevent collision and obstacle avoidance issues during the cooperative motion paths of multi-agent systems, this study adopts an individual-based Lagrangian modeling framework. The behavior of the group is understood as the result of interactions, where individuals attract each other when far apart and repel each other when close. This ensures a safe distance is maintained between individuals, accounting for the physical space occupied by each individual. Specifically, individuals attract each other at longer distances and repel at shorter distances. Modeling static and dynamic obstacles in the environment effectively captures the fundamental motion characteristics of biological groups in nature, ensuring a safe distance between individuals to avoid collisions during movement. In the collective motion of intelligent groups, the trajectory generated by the dynamics model of any individual serves as a reference trajectory for other agents to follow or track. This approach ensures coordinated path tracking and maintains orderly movement within the entire intelligent group system.

3. Construction of differential dynamics model for multi-agent coordinated motion

3.1 Multi-agent distribution of Lyapunov method

In the study of multi-agent systems, stability analysis is crucial. Lyapunov indirection is to introduce Lyapunov functions with generalized energy properties, and then analyze the monotonicity of the function by means of derivation, and then judge its stability. Suppose there is a nonlinear system of equations: In a system where the position, velocity, and acceleration of a multi-agent are jointly described, so that $f(x_e)=0$ satisfies in the neighborhood δ of the equilibrium point x_e . If a continuously differentiable positive definite function $V(x)$ defined in the neighborhood δ of x_e can be found, and satisfies in the neighborhood δ of the equilibrium point x :

$$\dot{V}(x) = \frac{\partial V}{\partial x} \frac{dx}{dt} < 0, x \in \delta \quad (2)$$

This equilibrium point is called a globally asymptotically stable equilibrium point, which means that no matter how far the initial state of the system is from the equilibrium point, the system will eventually tend to this equilibrium point as time evolves.

3.2 Modeling of multi-agent systems

3.2.1 Modeling principles and ordinary differential models

Taking the heat equation as an example, the position of the agent can be represented by the state variable $u(t, a)$, where the real part represents the horizontal coordinate and the imaginary part represents the vertical coordinate. There are multiple agents distributed in a two-dimensional plane. In order to achieve the formation goal of the multi-agent system in the plane, the multi-agent system constructed with an ordinary differential model usually uses (x, y) to represent the position of each agent. For the agents in the plane, the consistency control law is:

$$\dot{x}_i = \sum_{j \in \delta_i} a_{ij} (x_j - x_i) \quad (3)$$

$$\dot{y}_i = \sum_{j \in \delta_i} a_{ij} (y_j - y_i) \quad (4)$$

Each agent can only exchange information with other agents within its communication range, and these interactive agents constitute δ_i . a_{ij} represents the connection weight between agents i and j , reflecting the intensity of information interaction between the two agents^[6].

3.2.2 Partial differential equation modeling and collective dynamics model

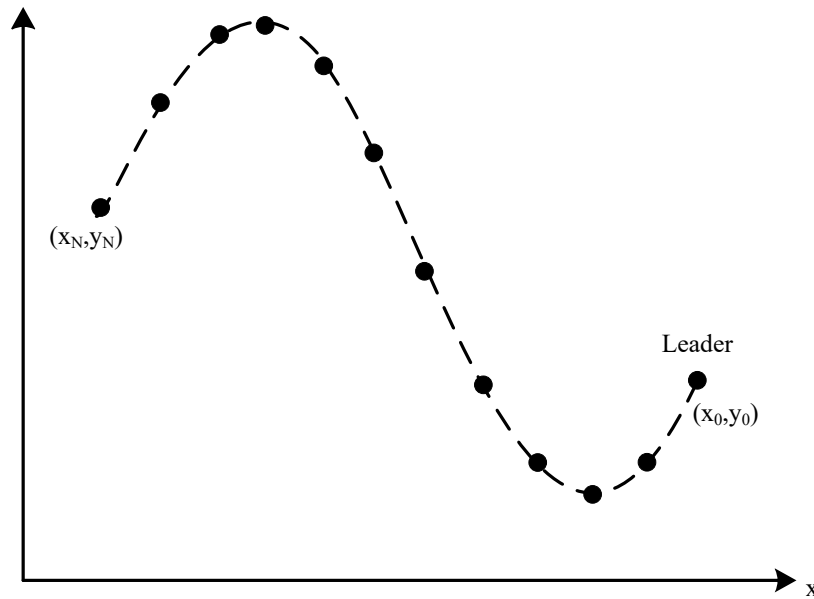
The originally discrete multi-agents are mapped to continuous space. By introducing the state variable $u(t, a) = x(t, a) + iy(t, a)$, the real part is used to represent the horizontal coordinate position of the agent, and the imaginary part represents the vertical coordinate position^[7-8]. Collective differential dynamics model of multi-agents:

$$u_i(t, a) = k_a [u_{aa}(t, a) - u_{aa}^d(t, a)] \quad (5)$$

Among them, $u_t = \frac{\partial u}{\partial t}$ reflects the change of the agent state over time; $u_{aa} = \frac{\partial^2 u}{\partial a^2}$ reflects the changing trend of the agent state in

spatial distribution; k represents the control gain, which determines the response intensity of the system to the deviation; $u^d(a)$ represents the expectation function, which can be set to achieve complex formations in collective formation motion tasks. The cooperative motion of a multi-agent system is illustrated in Figure 2. By adjusting the desired function, the multi-agent system can be configured into various specific shapes. Notably, in this study, the partial differential equation modeling and collective dynamics model frequently employ a leader-follower algorithm for multi-agent formations. This algorithm enables precise positioning within the system, with predesignated leader drones equipped with advanced navigation and mapping devices to acquire global information and continuously adjust their direction, position, and speed. Other agents move solely based on the leader's information, achieving the cooperative motion of the entire multi-agent system.

Figure 2 Coordinated motion of a multi-agent system



4. Simulation analysis and result discussion

4.1 Simulation platform and experimental setting

This study used a simulation platform based on MATLAB/Simulink for experiments. Table 1 shows the experimental environment, which lists the specific information of the computer hardware configuration and software environment used for simulation.

Table 1 Experimental environment

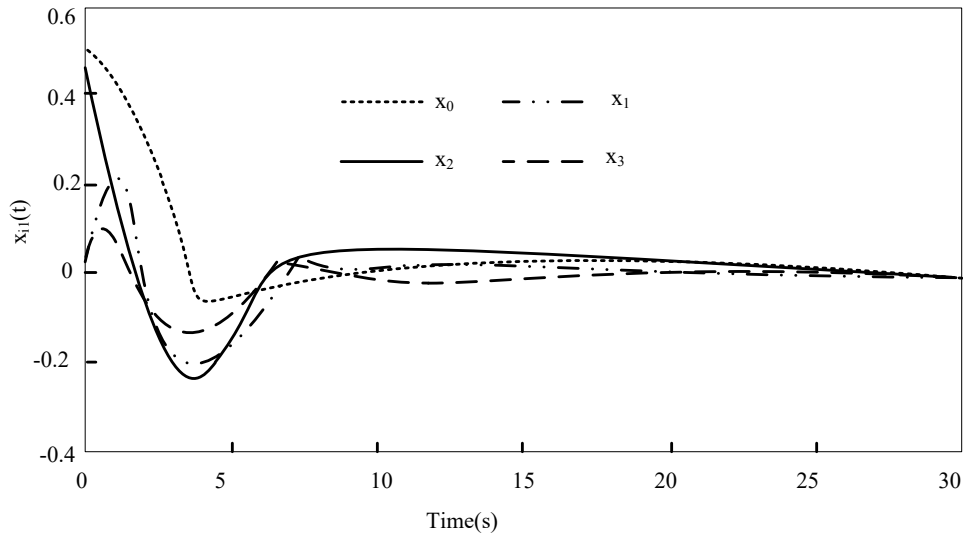
	Project	Configuration and description
Hardware Configuration	Intel Core i7-10700K, 8 cores and 16 threads, 3.8 GHz	Intel Core i7-10700K, 8 cores and 16 threads, 3.8 GHz
	32 GB DDR4 3200 MHz	32 GB DDR4 3200 MHz
	NVIDIA GeForce RTX 3060 12GB	NVIDIA GeForce RTX 3060 12GB
	1TB NVMe SSD	1TB NVMe SSD
	Windows 10 Pro 64-bit	Windows 10 Pro 64-bit
Software Configuration	MATLAB R2023b, Simulink 2023b	MATLAB R2023b, Simulink 2023b
	Control System Toolbox, Optimization Toolbox, Reinforcement Learning Toolbox, ADP Toolbox	Control System Toolbox, Optimization Toolbox, Reinforcement Learning Toolbox, ADP Toolbox
	Simulink for multi-agent system modeling, Stateflow for control flow and logic design	Simulink for multi-agent system modeling, Stateflow for control flow and logic design
	MATLAB, Simulink (graphical modeling)	MATLAB, Simulink (graphical modeling)
Simulation Settings	0.01 s	0.01 s
	50 s	50 s

4.2 Analysis of multi-agent cooperative motion trajectory

It can be seen that in the differential dynamics model of cooperative motion of agents using the proposed Lyapunov function method, the system states of all agents can reach a consensus with the leader node after about 10 seconds, as shown in Figure 3. Figure 3 (a) shows the position motion state of the agent. It can be seen that at the initial moment, the x_1 - x_0 states of agents with different numbers (including leaders and followers) have different starting values; at 4 seconds, x_1 is at -0.18, x_2 is at -0.20, x_3 is at -0.22, and x_0 is at 0.13, reflecting the initial differences in the states of the four individual agents. As time goes on, at a time node of about 9.5 seconds, the position motion states of the four individual agents tend to a common value of 0, and the state of the leader x_0 has completely served as the reference target state of other agents x_2 - x_4 . Figure 3 (b) shows the directional motion state of the agent. Similarly, the directional motion state values of each agent are different at the beginning. At 3 seconds, x_1 is in the direction of -0.19, x_2 is in the direction of -0.31, x_3 is in the direction of -0.39, and x_0 is in the direction of 0.20, which also shows the initial difference in the states of the four individual agents. As time gradually increases from 0 seconds, at about 7.8 seconds, the directional motion state curves of all agents gradually converge to the same, indicating that the system states of all agents reach a consensus with the leader node at this point in time, further proving the effectiveness of collaborative tracking.

Figure 3 Trajectories of four individual agents over time

(a) Position motion state trajectory of the agent



(b) Trajectory of the directional motion state of the agent

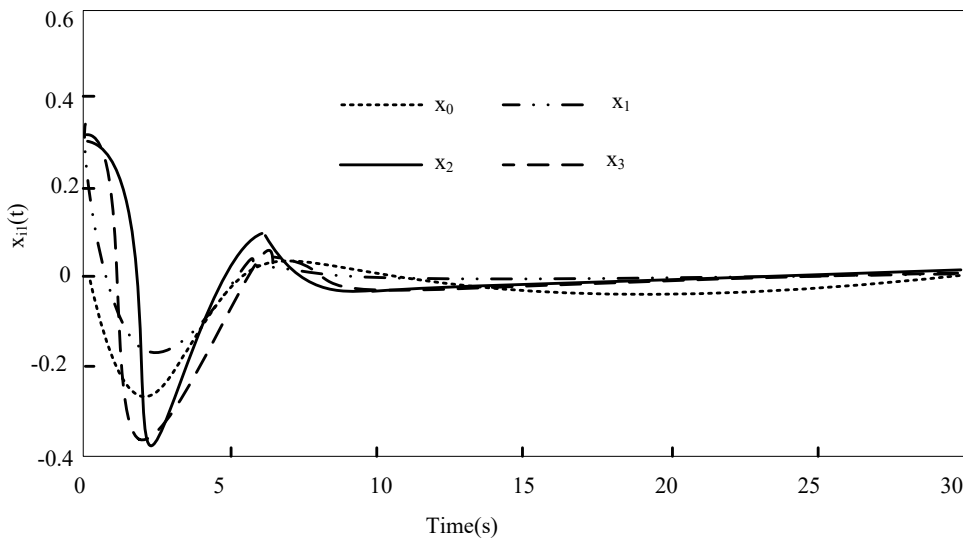
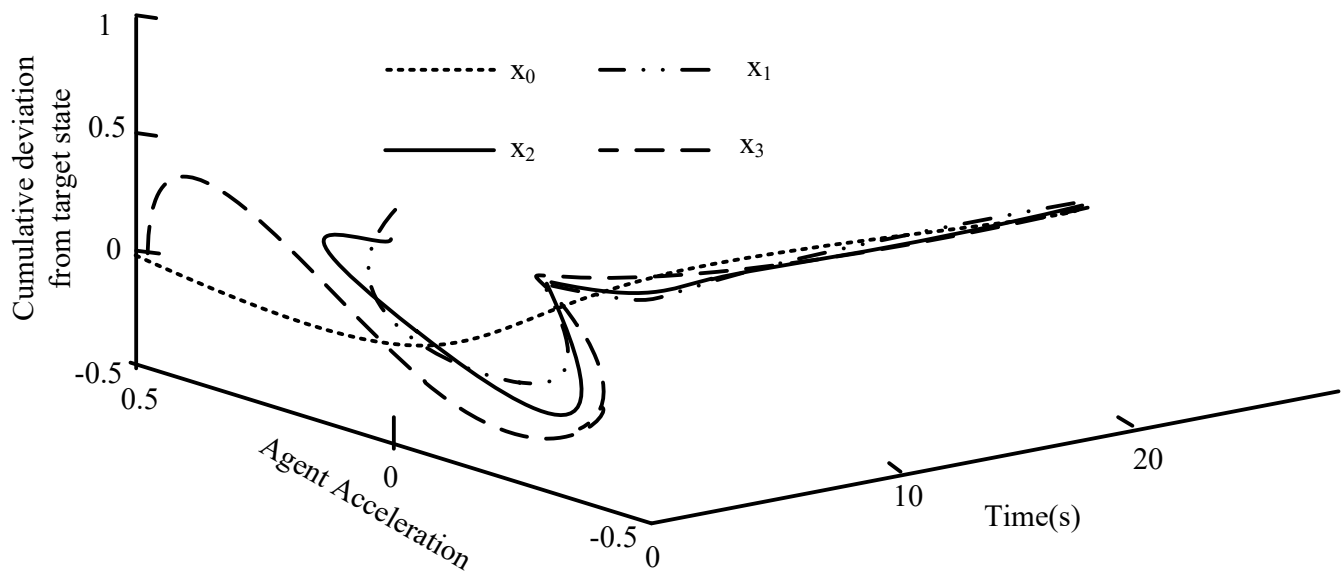


Figure 4 is a comprehensive evolution of the states of four individual agents, showing the overall situation of the agent acceleration of all agents (including leaders and followers) and the cumulative deviation of the agent from the target state. As shown in Figure 4, it can be seen that at the initial moment of the agent acceleration, the x_1 - x_0 states of agents with different numbers (including leaders and followers) have different starting values; at 3 seconds, the acceleration change rate of each agent may be large and different. x_1 is -0.16 acceleration, x_2 is -0.22 acceleration, x_3 is -0.25 acceleration, x_0 is at 0.19 acceleration, and when it finally reaches 8.2 seconds, the acceleration change rate tends to 0, ensuring the stability and coordination of the agent's movement. It reflects the initial differences in the states of the four individual agents. Then observe the cumulative deviation between the agent and the target state. In the initial stage, the distance between each agent and the target state is different. As time goes by, the agent keeps approaching the target state. At about 10 seconds, the cumulative deviation gradually decreases, and the desired collaborative state is achieved, indicating that all agents have successfully reached a state consensus. The effectiveness and stability of the method in this paper are demonstrated.

Figure 4. The evolution of the states of four individual agents



4.3 Comparison of multi-agent collaborative motion performance

In order to further verify the motion performance of each agent in the multi-agent system of this method, this paper selects three common traditional PID control methods, consensus algorithms, and distributed control methods for comparative analysis. Table 2 shows the performance comparison of the four methods in a dynamic warehousing environment. It can be seen that the multi-agent collaborative motion performance of the traditional PID control method is poor, and it cannot cope well with the complex dynamic adjustment when the formation shape changes. The number of path nodes is 26 nodes, the number of obstacle collisions is 16 times, the number of turning points is 12 times, and the calculation time is 64.5 seconds. In contrast, the consistency algorithm and the distributed control method have improved in some indicators, but there are still shortcomings. Although the consistency algorithm reduces the number of path nodes by 18 and the number of collisions with obstacles by 3 times, the calculation time of 59.2 and the number of path turning points of 11 are still relatively high. The distributed control method is further optimized in the number of path nodes (15) and the number of collisions with obstacles (2 times). This is because the distributed control method uses graph theory to describe the communication topology between multi-agents to complete the collaborative control of multi-agents, but it is also slightly lower than the traditional method. However, the proposed method showed significant advantages in all indicators. The number of path nodes was reduced to only 6, the number of path turning points was kept at a reasonable 5, and no obstacle collisions occurred, which greatly improved the safety and efficiency of the operation. The calculation time was also shortened to 49.6 seconds, which is better than all other methods. The proposed method performed best in the dynamic environment method, with higher efficiency and

safety of moving group path planning, and is a better collaborative strategy.

Table 2 Performance comparison of four methods in dynamic storage environment

Method	Path Node	Collision frequency	Turning Points	Calculation time /s
Traditional PID control method	26	8	12	64.5
Consistency algorithm	18	3	11	59.2
Distributed control method	15	2	7	58.6
This method	6	0	5	49.6

5. Conclusion

This study employs a Lyapunov indirect method to establish a multi-agent system model based on partial differential equations (PDEs). Initially, the system's dynamic obstacle avoidance and real-time response capabilities in formation tracking were not provided. Subsequently, the stability of the system was determined by analyzing the eigenvalue distribution of the linear system state equation. By mapping the originally discrete multi-agent system into a continuous space using PDEs, the control accuracy and efficiency of the cooperative motion system were improved. Simulation results verified the effectiveness of the proposed method.

In the trajectory analysis of cooperative motion, the position, direction acceleration, and cumulative deviation of four individual agents relative to the target stabilized within 9.5 seconds, 7.8 seconds, 8.2 seconds, and 10 seconds, respectively. The motion states converged toward a common value of 0, achieving overall stability through unified cooperative changes. Moreover, no obstacle collisions occurred, and the computation time of 49.6 seconds was significantly shorter compared to three other methods. This demonstrates the method's high efficiency and quality in achieving cooperative tracking, formation, and obstacle avoidance behaviors among agents.

Funding

no

Conflict of Interests

The author(s) declare(s) that there is no conflict of interest regarding the publication of this paper.

References

- [1] Amirkhani A, Barshooi A H. Consensus in multi-agent systems: a review[J]. Artificial Intelligence Review, 2022, 55(5): 3897-3935.
- [2] Wang J, Hong Y, Wang J, et al. Cooperative and competitive multi-agent systems: From optimization to games[J]. IEEE/CAA Journal of Automatica Sinica, 2022, 9(5): 763-783.
- [3] Bao G, Ma L, Yi X. Recent advances on cooperative control of heterogeneous multi-agent systems subject to constraints: A survey[J]. Systems Science & Control Engineering, 2022, 10(1): 539-551.
- [4] Ren H, Wang Y, Liu M, et al. An optimal estimation framework of multi-agent systems with random transport protocol[J]. IEEE Transactions on Signal Processing, 2022, 70: 2548-2559.
- [5] Liu Y, Liu J, He Z, et al. A survey of multi-agent systems on distributed formation control[J]. Unmanned Systems, 2024, 12(05): 913-926.
- [6] Yu C, Velu A, Vinitzky E, et al. The surprising effectiveness of ppo in cooperative multi-agent games[J]. Advances in Neural Information Processing Systems, 2022, 35: 24611-24624.
- [7] Fang Z, Jiang D, Huang J, et al. Autonomous underwater vehicle formation control and obstacle avoidance using multi-agent generative adversarial imitation learning[J]. Ocean Engineering, 2022, 262: 112182.
- [8] Li J, Shi H, Guo Y, et al. Tragcan: Trajectory prediction of heterogeneous traffic agents in iov systems[J]. IEEE Internet of Things Journal, 2022, 10(8): 7100-7113.

The Nonlinear Mathematical Modeling and Optimization of Distributed Control in Complex Systems

Shao Qiang*

Gaston Day School Shanghai Shangde, Shanghai 201315, China

*Corresponding author: Shao Qiang, sost12822@163.com

Copyright: 2025 Author(s). This is an open-access article distributed under the terms of the Creative Commons Attribution License (CC BY-NC 4.0), permitting distribution and reproduction in any medium, provided the original author and source are credited, and explicitly prohibiting its use for commercial purposes.

Abstract: With the widespread application of complex systems in industries such as manufacturing, transportation, and energy, their high-dimensional, strongly nonlinear, and dynamically coupled characteristics pose significant challenges to traditional centralized control. To address these complexities more efficiently, this study constructs a nonlinear mathematical model by introducing nonlinear feature mapping into a multiple linear regression framework and implements distributed optimization using the Alternating Direction Method of Multipliers (ADMM). The proposed method is validated through the simulation of the nonlinear dynamic behavior of a deep-water riser–test pipe system, with experimental designs encompassing multi-dimensional vibration responses and dynamic environmental disturbances. The results demonstrate that the proposed nonlinear model significantly outperforms other methods in terms of prediction accuracy and optimization efficiency. Under varying amplitudes and frequencies of disturbances, the model achieves lower error rates and higher robustness, with an adaptation decay rate of less than 17.6%. These findings indicate that the proposed nonlinear modeling and distributed optimization approach can effectively capture the dynamic characteristics of complex systems, making it suitable for real-time distributed control scenarios with promising engineering applications.

Keywords: Complex Systems; Multiple Linear Regression Model; Nonlinear Features; Distributed Optimization; Optimization Efficiency.

Published: Jan 14, 2025

DOI: <https://doi.org/10.62177/jaet.v2i1.152>

1. Introduction

With the continuous development of science and technology, the application of complex systems in industries such as manufacturing, transportation, energy, and information technology has been expanding rapidly ^[1]. These systems are often characterized by high dimensionality, strong nonlinearity, dynamic coupling, and multiple constraints, making traditional centralized control methods increasingly inadequate to meet practical needs. Due to its flexibility, scalability, and computational parallelization, distributed control has emerged as a key research focus for the control of complex systems ^[2]. However, research on distributed control in complex systems still faces many challenges. The dynamic relationships and nonlinear coupling characteristics within complex systems are highly intricate, and traditional mechanism-based analytical methods often struggle to construct mathematical models that align with real-world scenarios. This frequently results in decreased control performance and computational efficiency. Additionally, some optimization methods exhibit high computational complexity when addressing distributed nonlinear systems, making them unsuitable for real-time control requirements. Consequently, constructing efficient and accurate nonlinear mathematical models combined with advanced

optimization algorithms has become a core research direction in addressing the distributed control problems of complex systems^[3].

In this context, leveraging large-scale data processing technologies widely applied in complex systems allows the modeling of system dynamics through data-driven approaches. Distributed optimization algorithms can further enhance the performance and efficiency of control systems. By designing well-constructed nonlinear mathematical models, it becomes possible not only to capture the nonlinear dynamic characteristics within systems but also to provide theoretical support and engineering guidance for real-time fault prediction and parameter optimization in complex systems. Such methods can effectively identify potential risk factors, enable early parameter adjustments, reduce the risk of control system failures, and provide reliable technical means to ensure the safety and efficient operation of systems.

2. Nonlinear mathematical modeling and optimization

2.1 Nonlinear mathematical modeling strategy

In complex systems, due to the highly nonlinear coupling relationships between internal variables, directly establishing precise mathematical models is often challenging. However, by applying appropriate linear transformations to nonlinear systems, certain nonlinear problems can be converted into analytically solvable linear problems, thereby simplifying the modeling and solution process^[4-5]. This approach is widely used in nonlinear regression modeling, where constructing suitable feature spaces or performing variable transformations enables the simplification of originally complex nonlinear relationships into linear forms.

Taking into account the linear transformation within nonlinear systems, a standard representation of a nonlinear system model is given as:

$$\begin{aligned} y(k) &= f(y(k-1), \dots, y(k-n), \\ &u(k-1-k_d), \dots, u(k-n-k_d)) + d(k) \end{aligned} \quad (1)$$

Where: $f(\bullet)$ represents the unknown linear function, $u(\bullet) \in R^m$ is the control input vector, $y(\bullet) \in R^q$ is the system output vector, n_u and n_y denote the input and output orders. k_d is the delay and $d(k)$ is the noise. The nonlinear system's mathematical model operates in a rolling manner. At each sampling time k , a nonlinear optimization problem needs to be solved online to obtain the control effect. Assuming the constraint optimization performance index $J(k)$ at time k is defined as:

$$\begin{aligned} J(k) &= \frac{1}{2} \sum_{h=1}^{N_p} [r(k+h|k) - y(k+h|k)]^2 + \\ &\frac{1}{2} \sum_{h=1}^{N_u} q_h \Delta u^2(k+h-1|k) \end{aligned} \quad (2)$$

The constraints are:

$$u_{\min} \leq u(k+h-1|k) \leq u_{\max} \quad (3)$$

$$\Delta u_{\min} \leq \Delta u(k+h-1|k) \leq \Delta u_{\max} \quad (4)$$

$$y_{\min} \leq y(k+h|k) \leq y_{\max} \quad (5)$$

Where: $r(k+h|k) \in R^q$ is the expected output of the h th step starting from sampling time k , and $y(k+h|k) \in R^q$ is the predicted output of the h th step starting from sampling time k .

And the control increment is:

$$\Delta u(k+h-1|k) = u(k+h-1|k) - u(k+h-2|k) \quad (6)$$

Where: N_p and N_u represent the prediction and control time domains, respectively. q_h is the control weight coefficient, u_{\max} and u_{\min} define the bounds of $u(k+h-1|k)$. Δu_{\max} and Δu_{\min} specify the bounds of $\Delta u(k+h-1|k)$. y_{\max} and y_{\min} are the upper and lower bounds of $y(k+h|k)$.

Distributed control in complex systems needs to address highly coupled nonlinear dynamic characteristics, and nonlinear mathematical modeling serves as the core foundation for achieving efficient control. Multiple linear regression models demonstrate strong capabilities in handling large-scale data computation and prediction, and they can capture nonlinear relationships within systems by introducing nonlinear features or variable transformations. Therefore, based on multiple linear regression models, we can integrate nonlinear feature expansions or other nonlinear transformation methods to construct nonlinear mathematical models suitable for complex systems. This enables better characterization of the system's dynamic behavior and optimization of control performance.

2.2 Model Optimization

In the distributed control of complex systems, model optimization is a critical step in enhancing system performance and achieving efficient control. Generally, optimization strategies for nonlinear mathematical models can be broadly categorized into two types: model optimization methods based on physical mechanisms and data-driven model optimization methods.

2.2.1 Mechanism-based model optimization

The mechanism-based analysis method relies on an in-depth understanding of system characteristics, analyzing causal relationships and extracting the internal mechanism of the system to construct a mathematical model with clear physical significance. Models optimized using this method typically have high interpretability and applicability, making them more suitable for achieving collaborative optimization in distributed control systems.

During the model optimization process, it is essential to first clarify the system context and modeling objectives. This involves analyzing the actual operational background of the complex system and defining the primary goals of model optimization, such as improving prediction accuracy, reducing computational complexity, or enhancing real-time performance. Based on the system's characteristics, reasonable simplifications and assumptions should be made, discarding secondary factors and emphasizing the role of key variables. This process requires combining the system's underlying mechanisms with data analysis to extract critical features, ultimately linearizing or nonlinearizing the problem to provide support for subsequent optimization.

The focus of model optimization lies in the rational construction of nonlinear relationships, analyzing the causal relationships among system variables, and designing mathematical structures that align with real-world scenarios by integrating the system's mechanisms. In distributed control, the model must undergo error analysis and robustness verification to ensure its stability and accuracy during actual operation.

2.2.2 Data-driven model optimization

For complex systems characterized by strong nonlinearity, time variability, and uncertainty, data-driven model optimization methods have increasingly become a significant research focus. Unlike traditional mechanism-based approaches, data-driven methods directly construct or optimize nonlinear mathematical models by collecting and processing large amounts of system operation data, thereby enhancing system prediction capabilities and control effectiveness. By analyzing data, these methods identify key variables that critically influence system control while eliminating irrelevant factors to reduce modeling complexity. Optimization algorithms are employed to dynamically adjust the parameters of the nonlinear model, improving its adaptability and accuracy [6]. During model operation, continuous error analysis is conducted, and dynamic optimization is performed based on distributed feedback mechanisms. By improving the model structure or refining the optimization algorithm, the model can more accurately predict the system's dynamic behavior. This reduces model-solving time and meets the real-time requirements of distributed control systems. Additionally, through error analysis and model adjustments, the model maintains stability in complex and dynamic environments.

2.2.3 Optimize the process

The nonlinear mathematical modeling and optimization of distributed control in complex systems require a combination of mechanism-based analysis and data-driven approaches, with continuous optimization built on the foundation of model construction. Through reasonable simplifications, error correction, and the application of distributed optimization algorithms, the prediction accuracy and control performance of the model can be effectively enhanced, providing strong support for distributed control in complex systems. Figure 1 illustrates the optimization process, which proceeds as follows:

(1)Data Collection and Preprocessing

Collect large amounts of sample data from the complex system, including input vectors, state variables, and output results. Clean and preprocess the data by removing outliers, filling in missing values, and normalizing the data to improve quality.

(2)Initial Model Construction

Use data-driven methods or mechanism-based approaches to construct an initial nonlinear mathematical model. Introduce specific nonlinear feature mappings into the model to describe the system's nonlinear dynamic characteristics.

(3)Parameter Optimization

Apply fitting algorithms to perform an initial optimization of the model parameters to obtain output results. Continuously adjust input vectors, control output vectors, and calculate the model's predictions.

(4)Model Validation

Compare the prediction results with expected values, calculate errors, and analyze their sources. Validate the model's rationality and applicability and assess its performance in real-world systems.

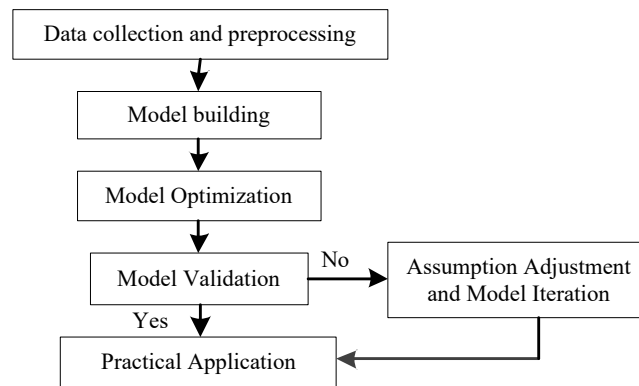
(5)Assumption Adjustment and Iterative Improvement

Based on validation results, check for deficiencies in the model assumptions. If the model does not fully meet practical requirements, revise or supplement the assumptions and rebuild the model. Through multiple rounds of optimization and adjustments, progressively refine the model until the prediction results achieve the desired accuracy.

(6)Application in Distributed Control

Apply the final optimized nonlinear mathematical model to distributed control systems for real-time prediction, fault detection, or resource allocation. Dynamically update the model parameters during operation to adapt to system changes.

Figure 1 Optimization process



3 Experimental results and analysis

In complex systems, nonlinear mathematical modeling and optimization of distributed control usually require experimental verification of the effectiveness of modeling and the applicability of the optimization process. In order to verify the advantages of the constructed nonlinear mathematical model in terms of prediction accuracy and optimization performance, this paper designs a distributed vibration control experiment based on the dynamic behavior of complex systems.

3.1 Experimental Configuration

The experiment selected dynamic vibration control in complex systems as the research object, simulating the nonlinear dynamic behavior of the deepwater riser-test pipe system to verify the prediction accuracy and optimization effect of the nonlinear mathematical model. The system structure is shown in Figure 2. The riser subsystem includes vibration behaviors in the cross-flow direction and the downstream direction, which is used to simulate the dynamic impact of environmental disturbances on complex systems. The test pipe subsystem includes vibration responses in the downstream and upstream directions, which is used to simulate the dynamic coupling relationship between multiple subsystems.

3.2 Experiment variable settings

The vibration frequency is the output variable of the system, which is used to measure the dynamic response of the riser-test tube system under external disturbance. In this experiment, the vibration frequency range is set to 0.5Hz to 10Hz to cover

the common low-frequency vibration characteristics in deepwater environments. The data sampling frequency is 1000Hz to ensure the capture of the detailed characteristics of the system vibration process. The independent variable setting includes the response quantities in four vibration directions, and the specific ranges are as follows:

- (1) Transverse vibration is the reflection of the lateral force of the fluid on the riser, which is mainly caused by waves and lateral disturbances of the fluid. In the experiment, the displacement range of transverse vibration is set to $\pm 10\text{mm}$, the initial vibration frequency is 2Hz, and the disturbance intensity gradually increases.
- (2) Streamwise vibration reflects the movement characteristics of the riser in the direction of water flow, and the displacement range is set to $\pm 15\text{mm}$, and the corresponding disturbance frequency is 1Hz to 5Hz.
- (3) Streamwise vibration is mainly affected by the coupling effect of the riser vibration, and the displacement range is $\pm 12\text{mm}$. During the test, the flow rate is gradually increased (0.5m/s to 1.5m/s) to analyze the coupling effect under different flow conditions.
- (4) The countercurrent vibration is mainly caused by fluid backflow disturbance, with a displacement range of $\pm 8\text{mm}$, and the corresponding flow rate range is set to 0.3m/s to 1.2m/s.

To ensure the environmental consistency and rationality of the structural characteristics of the experiment, Table 1 shows the specific parameters of the auxiliary variables. Fluid density and flow rate are the key control variables of the experiment, which directly affect the vibration response characteristics of the riser and test pipe. The length, diameter and stiffness coefficient of the riser and test pipe comprehensively reflect the physical characteristics of the experimental system. The experiment lasted for 60s, combined with a sampling frequency of 1000Hz, which can ensure that dynamic data is collected for a long enough time. The high-frequency sampling rate can also capture the subtle vibration changes of the system under complex dynamic conditions.

Table 1 Specific parameters of auxiliary variables

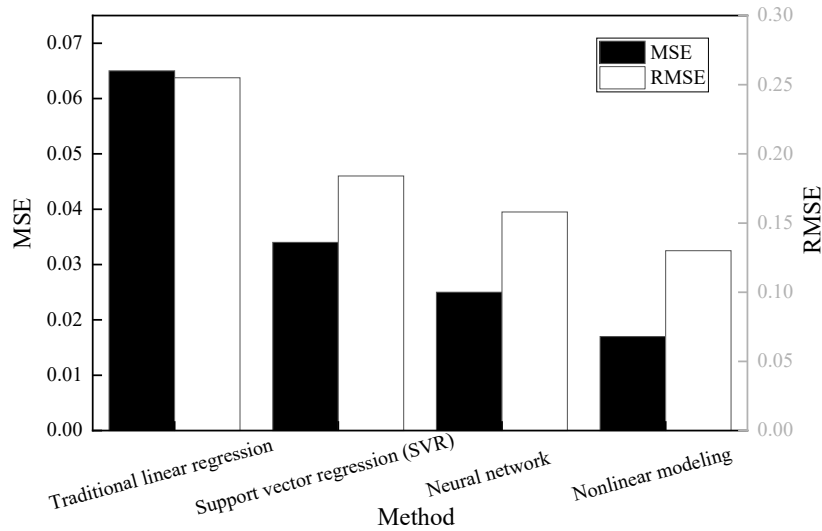
Category	Variable name	Numeric
Environmental parameters	Fluid density	1025 kg/m ³
	Flow rate	0.3 m/s-1.5 m/s
	Fluid temperature	10°C -20°C
Structural parameters	Riser length	100 m
	Riser diameter	0.5 m
	Riser stiffness factor	2000 N/m
	Test tube length	80 m
	Test tube diameter	0.3 m
	Test tube stiffness factor	1500 N/m
Time Dimension	Duration of each experiment	60s
	Data sampling frequency	1000 Hz
	Number of data sampling points	60000

3.3 Results Analysis

3.3.1 Prediction Error

The data collected in the experiment contains 60,000 records, which are derived from the time series data of each experiment. The sampling frequency is 1000 Hz and the experiment duration is 60 s. Figure 3 shows the model prediction accuracy evaluation, using mean square error (MSE) and root mean square error (RMSE) as the main evaluation indicators. Compared with the traditional linear regression model, the proposed nonlinear mathematical model has an MSE and RMSE of 0.017 and 0.130, respectively, which significantly improves the prediction accuracy. Compared with SVR and neural network, the MSE and RMSE of the proposed method are reduced, indicating that the model is superior in capturing nonlinear characteristics. The proposed nonlinear modeling method can efficiently capture the nonlinear dynamic characteristics of the system in complex systems, while having both prediction accuracy and computational efficiency, and is very suitable for the design and optimization of real-time distributed control systems.

Figure 3 Model prediction accuracy evaluation



3.3.2 Optimizing efficiency

In the nonlinear modeling of distributed control in complex systems, the convergence speed and computation time of optimization algorithms are key metrics for evaluating their efficiency. This experiment compares the proposed nonlinear mathematical model with traditional linear regression, support vector regression (SVR), and neural networks. Table 2 presents the results of the optimization efficiency comparison. The proposed nonlinear mathematical model achieves optimization with the fastest convergence speed, requiring only 30 iterations to meet the convergence condition. In contrast, traditional nonlinear regression models require 150 iterations, and the step size for each update must be carefully adjusted; otherwise, issues such as oscillations or slow convergence may arise. SVR and neural networks require 50 and 100 iterations, respectively, and while both perform well in handling nonlinear problems, their heuristic optimization methods lead to slower convergence processes due to the randomness of the initial population.

The proposed nonlinear mathematical model has a total computation time of 10.2 seconds, significantly outperforming other methods and demonstrating the notable advantages of distributed optimization under parallel computation. Although traditional nonlinear regression models involve simpler computations, their excessive iteration count results in a total time of 28.5 seconds. SVR and neural networks require 18.7 seconds and 33.4 seconds, respectively, as their computation involves extensive population updates and fitness evaluations, leading to higher computational complexity. The significant advantages of the proposed nonlinear mathematical model in terms of convergence speed and computation time, as validated through comparisons with other optimization methods, highlight its superiority in nonlinear modeling and optimization for complex systems.

Table 2 Comparison results of optimization efficiency

Method	Convergence iterations	Convergence time/s	Calculate total time/s
Traditional linear regression	150	6.8	28.5
Support vector regression (SVR)	50	4.2	18.7
Neural network	100	7.6	33.4
Nonlinear modeling	30	2.5	10.2

3.3.3 Robustness

To evaluate the model's adaptability under different input disturbances, the experiment introduced noise with varying amplitudes and frequencies into the test data to simulate real-world input disturbances. The disturbance amplitudes were set at $\pm 5\%$, $\pm 10\%$, and $\pm 15\%$ of the input signal values, representing mild, moderate, and severe disturbances. The results of the anti-disturbance capability test are shown in Table 3. For the nonlinear modeling method, the MSE under low-amplitude disturbances was only 0.020, close to 0.017 in the undisturbed scenario, with an adaptation decay rate (AR) of 17.6%,

demonstrating strong robustness. In contrast, the MSE for traditional linear regression increased rapidly under disturbance conditions, reaching 0.130 at $\pm 15\%$ amplitude and 10 Hz frequency, indicating poor adaptability to nonlinearity and disturbances. Under all disturbance conditions, the AR of the nonlinear modeling method was significantly lower than that of traditional linear regression and SVR, showing its superior ability to handle input disturbances. The nonlinear modeling method effectively reduces the impact of input disturbances on prediction results, maintaining high prediction accuracy, especially under low-amplitude disturbances. This indicates strong robustness and adaptability for distributed control in complex systems. Traditional linear regression, due to its inability to capture nonlinear relationships, shows poor adaptability to disturbances and is unsuitable for complex dynamic environments. Although neural network methods demonstrate better adaptability, their low computational efficiency makes them less suitable for real-time control scenarios.

Table 3 Anti-interference ability test results

Method	Disturbance Amplitude	MSE (perturbation)	MSE (undisturbed)	Fitness decay rate (AR)
Traditional linear regression	$\pm 5\%$	0.06	0.045	33.30%
	$\pm 10\%$	0.095	0.045	111.10%
	$\pm 15\%$	0.13	0.045	188.90%
Support vector regression (SVR)	$\pm 5\%$	0.03	0.025	20.00%
	$\pm 10\%$	0.04	0.025	60.00%
	$\pm 15\%$	0.055	0.025	120.00%
Neural network	$\pm 5\%$	0.018	0.015	20.00%
	$\pm 10\%$	0.024	0.015	60.00%
	$\pm 15\%$	0.032	0.015	113.30%
Nonlinear modeling	$\pm 5\%$	0.02	0.017	17.60%
	$\pm 10\%$	0.026	0.017	52.90%
	$\pm 15\%$	0.034	0.017	100.00%

4. Conclusion

This study investigates the nonlinear mathematical modeling and optimization of distributed control in complex systems and proposes an efficient modeling method that combines nonlinear feature mapping with distributed optimization. Based on the experimental results, the following conclusions can be drawn:

- (1) The proposed nonlinear mathematical model, integrating feature mapping with multiple linear regression, effectively captures the nonlinear dynamic characteristics of complex systems. The MSE and RMSE reached 0.017 and 0.130, respectively, which are significantly better than those of traditional linear regression, SVR, and neural network methods.
- (2) The nonlinear mathematical model exhibits significant advantages in optimization speed and computational efficiency, requiring only 30 iterations to converge with a computation time of 10.2 seconds, far lower than SVR (18.7 seconds) and neural networks (33.4 seconds).
- (3) Under input signal disturbance conditions, the model demonstrates strong robustness. At a disturbance amplitude of $\pm 5\%$, the adaptation decay rate is 17.6%, which is significantly lower than that of other comparison methods.

The proposed nonlinear modeling and optimization approach combines prediction accuracy with computational efficiency, making it suitable for real-time control, fault prediction, and resource allocation scenarios in complex systems. It provides critical theoretical support for the engineering practices of distributed control.

Funding

no

Conflict of Interests

The author(s) declare(s) that there is no conflict of interest regarding the publication of this paper.

References

- [1] Chen X, Yang Z, Xu Y, et al. Progress and prediction of multicomponent quantification in complex systems with practical LC-UV methods[J]. *Journal of Pharmaceutical Analysis*, 2023, 13(2): 142-155.
- [2] D'Souza R M, di Bernardo M, Liu Y Y. Controlling complex networks with complex nodes[J]. *Nature Reviews Physics*, 2023, 5(4): 250-262.
- [3] Kičić I, Vlachas P R, Arampatzis G, et al. Adaptive learning of effective dynamics for online modeling of complex systems[J]. *Computer Methods in Applied Mechanics and Engineering*, 2023, 415: 116204.
- [4] Asghari M, Fathollahi-Fard A M, Mirzapour Al-E-Hashem S M J, et al. Transformation and linearization techniques in optimization: A state-of-the-art survey[J]. *Mathematics*, 2022, 10(2): 283.
- [5] Liu C, Zhu L, Belkin M. Loss landscapes and optimization in over-parameterized non-linear systems and neural networks[J]. *Applied and Computational Harmonic Analysis*, 2022, 59: 85-116.
- [6] Zhou Y, Zhang X, Ding F. Partially-coupled nonlinear parameter optimization algorithm for a class of multivariate hybrid models[J]. *Applied Mathematics and Computation*, 2022, 414: 126663.

A literature Review of Ant Colony Algorithm Based on Cite Space

Shiyu Li¹, Shengpan Yang², Jie Jin^{3*}

1. School of Logistics and Management Engineering, Yunnan University of Finance and Economics, Yunnan Kunming 650032, China;

2. Yunnan Provincial Institute of Geology and Mineral Surveying and Mapping, Yunnan Kunming 650032, China;

3. School of Finance and Public Administration, Yunnan University of Finance and Economics, Yunnan Kunming 650032, China)

*Corresponding author: Jie Jin, jinnie@ynufe.edu.cn

Copyright: 2025 Author(s). This is an open-access article distributed under the terms of the Creative Commons Attribution License (CC BY-NC 4.0), permitting distribution and reproduction in any medium, provided the original author and source are credited, and explicitly prohibiting its use for commercial purposes.

Abstract: Ant colony algorithm is a kind of biological heuristic algorithm, which has been applied in the fields of combinatorial optimization, path planning, task scheduling and other fields and has achieved significant optimization results, so it is necessary to sort out the literature of ant colony algorithm and deepen the understanding of its research status, hotspots and future development directions. In this paper, the process, principle and application fields of ant colony algorithm are sorted out, and the literature related to ant colony algorithm is bibliologically analyzed based on Cite Space software, and the number of publications, the current situation of researchers and research institutions are summarized, and the research hotspots and trends of ant colony algorithm are revealed through citation network and keyword co-occurrence analysis. Through bibliometric analysis, we understand that the research on ant colony algorithm is stable, and there is overlap and integration with other optimization algorithms. Future research can continue to focus on the improvement and application of ant colony algorithm, and explore its combination with other algorithms to promote the application of ant colony algorithm in a wider range of fields.

Keywords: Ant Colony Algorithm; Cite Space; Bibliometrics

Published: Feb 22, 2025

DOI: <https://doi.org/10.62177/jaet.v2i1.170>

1.Introduction

As a biological heuristic optimization algorithm, ant colony algorithm is inspired by ant foraging behavior, in nature, ants find the shortest path and optimal solution through collective behavior through pheromone release and perception. By simulating the pheromone communication and collective behavior of ant colonies, the ant colony algorithm introduces bio-inspired intelligence into the field of computing, and is committed to solving complex problems such as integrated circuit layout (Wu et al., 2022), path planning (Guo et al., 2023), combinatorial optimization (Hu et al., 2023), and image recognition (Shi et al., 2021). Compared with the limitations of traditional optimization methods, which are easy to fall into local optimum, the proposed algorithm can quickly search for the global optimal solution in the distributed self-organizing model with the help of positive feedback mechanism and pheromone guidance, which fills the technical gap of large-scale optimization problems (Yang et al., 2020). Although the early version had the defects of local convergence and “deadlock”, through

continuous improvement and algorithm “mutation”, it has shown strong potential in scenarios such as shortest path search for travel merchants, optimization of graph vertex coloring, route planning and resource allocation of logistics vehicles, and significantly shortened the time and cost (Yu et al., 2021). However, in the face of challenges such as dynamic environment adaptation, multi-objective constraint processing, and convergence efficiency improvement, current research still focuses on the in-depth optimization of algorithm performance (Xu Wei, 2023). Therefore, based on the Cite Space bibliometric method, this paper systematically reviews the theoretical development, research trends and application hotspots of ant colony algorithm, aiming to comprehensively understand the application status and development trend of ant colony algorithm in optimization problems, provide reference and inspiration for researchers, promote the application and development of ant colony algorithm in a wider range of fields and problems, and provide methodological reference for cross-domain optimization research.

2. Introduction to ant colony algorithms

2.1 The Proposal and Development of Ant Colony Algorithm

The development process of ant colony algorithm can be divided into four key stages:

1. Initial exploration (1992-1996): Proposed by Italian scholar Marco Dorigo in 1992, inspired by ants' foraging behavior, it was the first time to transform biological swarm intelligence into an optimal computing method. Although the initial theoretical framework did not receive much attention, Dorigo laid the foundation for the algorithm in 1996 by comparing traditional methods such as genetic algorithms to highlight its potential to solve complex optimization problems.
2. Theoretical improvement (1997-2003): The academic community focused on the deepening of core theories such as pheromone models and heuristic rules, and the first International Conference on Ant Colony Algorithm (ANTS'98) in 1998 promoted the research boom. In 2000, Bonabeau et al. published the first systematic review, and Gutjahr's team explored the convergence of algorithms from the perspective of graph theory.
3. Application Expansion (2004-2010): The algorithm verifies its effectiveness in combinatorial optimization scenarios such as traveling salesman problem and vehicle path planning, and its distributed optimization ability shows engineering value in the fields of logistics scheduling and task allocation, and promotes the transition of the algorithm from theory to practice.
4. Variant innovation (2011-present): The research has shifted to the direction of multi-objective optimization, adaptive parameter adjustment, etc., integrating local search strategies and other intelligent algorithms (such as particle swarm optimization) to improve performance. Derivative algorithms, such as the maximum-minimum ant colony system (MMAS) and multi-objective ant colony optimization (MOACO), have emerged one after another, which strengthens the robustness of the algorithms in dynamic environment and high-dimensional problems.

Over the past 30 years, the ant colony algorithm has gradually evolved from the initial idea of biological behavior simulation to a mature optimization tool with both theoretical depth and application breadth, and continues to drive innovation in the field of intelligent computing.

2.2 Principles of the ant colony algorithm

The ant colony algorithm dynamically optimizes path selection based on pheromone positive feedback and heuristic rules by simulating the cooperation mechanism of ant colonies. The core of the problem lies in the fact that ants construct solutions probably based on the pheromone concentration and heuristic information (such as path length) on the path, and strengthen the high-quality path by releasing pheromones to form a positive excitation. In the process of algorithm iteration, the pheromones are dynamically adjusted through the volatilization mechanism and the enhancement mechanism, so that the ant colony gradually converges to the global optimal solution in multiple searches. After the initial parameters are set, the ant continuously updates the path until the termination conditions are met, such as the maximum number of iterations or the solution quality is met, and finally realizes the efficient solution of complex combinatorial optimization problems through the self-organizing characteristics of swarm intelligence.

The transition probability of ant k moving from city i to city j at time t $P_{ij}^{(k)}$ formula is:

$$P_{ij}^{(k)} = \begin{cases} \frac{[\tau_{ij}(t)]^\alpha * [n_{ij}]^\beta}{\sum_{j \notin J_k} [\tau_{ij}(t)]^\alpha * [n_{ij}]^\beta}, & j \notin J_k \\ 0, & j \in J_k \end{cases} \quad (1)$$

In Eq. (1), $\tau_{ij}(t)$ is the concentration of the pheromone, n_{ij} is the heuristic, and is calculated as the reciprocal of the Euler distance from i to the j node, i.e.

$$n_{ij} = \frac{1}{d_{ij}} \quad (2)$$

When all ants complete the search, the pheromones on the path are updated with the following rules:

$$\tau_{ij}(t) = (1 - \beta)\tau_{ij}(t) + \Delta\tau_{ij} \quad (3)$$

In Eq. (3), β is the volatility coefficient, and $\Delta\tau_{ij}$ represents the increment of pheromones on the ij path, which is calculated as:

$$\Delta\tau_{ij} = \begin{cases} \frac{Q}{L_k}, & \text{When passing through } ij \\ 0, & \text{other} \end{cases} \quad (4)$$

In Eq. (4), L_k is the total length of the path taken by the k-th ant in this cycle, and Q is the total amount of pheromones released by the ant after completing a complete path search.

The specific steps of the ant colony algorithm are as follows:

1. Initialization: First, you need to initialize a set of ants and the relevant parameters of the problem. The initialization process includes determining the number of ants, the solution space of the problem, the initial value of pheromones, etc.
2. Ant path selection: Each ant chooses the next path according to the heuristic rules and pheromone concentration. Heuristic rules can be problem-related heuristics, such as path length, feasibility, and so on. Pathways with high pheromone concentrations are more likely to be chosen.
3. Construction and update of the solution: The ants select the path in turn and construct a solution according to the selected path. The construction of the solution can be sequential or parallel. After each ant selects the path, the pheromone is updated according to the quality of the solution, and the forward probability update method is generally used.
4. Pheromone update: After the ant selects the path, the pheromone will be updated. The renewal of pheromones follows the principle of pheromone volatilization and pheromone enhancement. Pheromone volatilization indicates that pheromones gradually decrease over time to prevent premature convergence. Pheromone enhancement indicates an increase in pheromone concentration based on the quality of the path chosen by the ant.
5. Judgment of termination conditions: After each iteration, it is necessary to judge whether the termination conditions are met. A common termination condition can be to reach the maximum number of iterations, to obtain a satisfactory solution, or to satisfy a problem-specific stopping condition.
6. Iterative update: If the termination condition is not met, the algorithm will continue to iteratively execute steps 2 to 5 until the termination condition is met.

3. Bibliometric analysis of ant colony algorithms

3.1 Data source

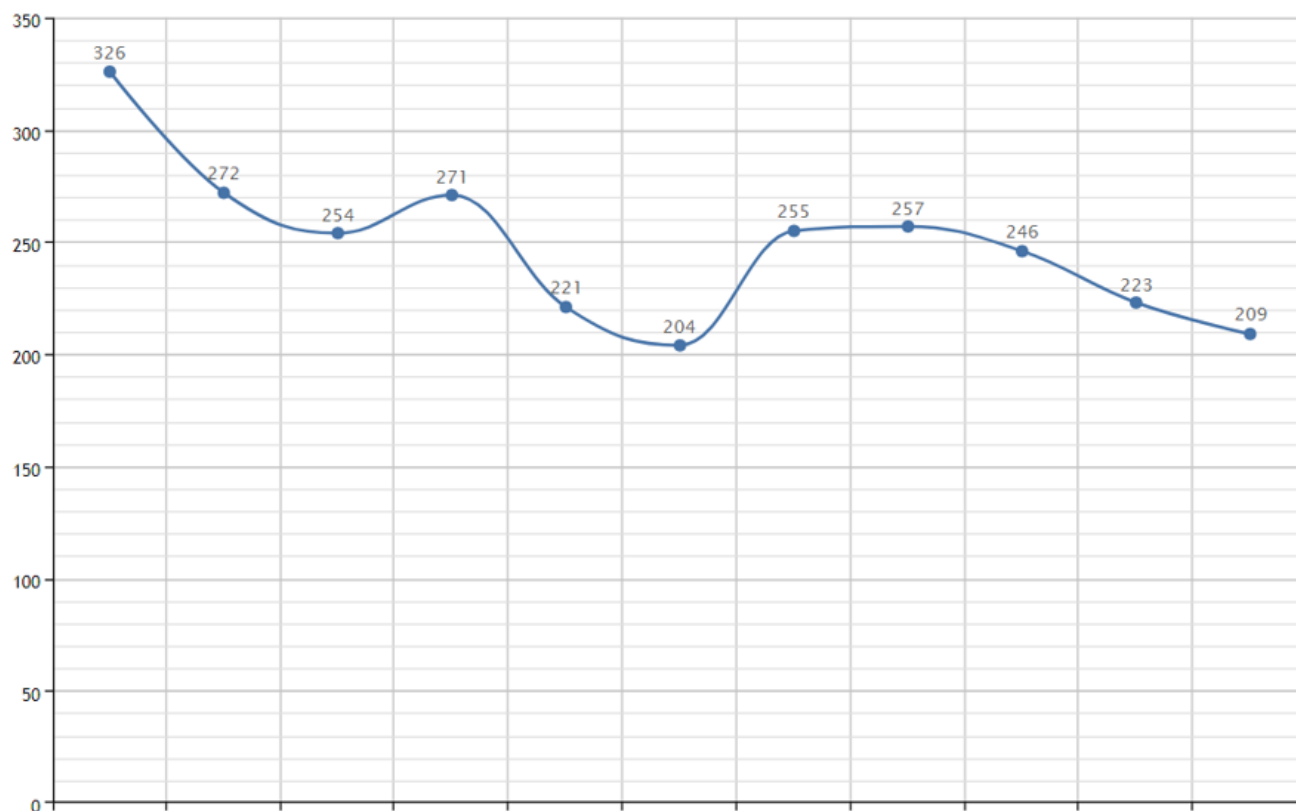
Cite Space is a powerful academic research tool designed by Dr. Chaomei Chen of Drexel University in the United States, focusing on the field of literature analysis and visualization. Built in the Java programming language, the software is designed to provide users with a high-performance platform to measure and explore the trajectory of specific academic fields. Through Cite Space, researchers are able to uncover the critical path of discipline evolution, and its core competency is to generate a series of intuitive graphs that help users deeply understand the dynamics and cutting-edge trends of the discipline. Cite Space is designed to help researchers explore knowledge structures, research hotspots, and academic trends in the field of academic research. It provides a wealth of features and tools that enable users to analyze and present bibliographic data in an intuitive and interactive way.

In this paper, “subject name = ‘ant colony algorithm’” was searched in the China Academic Journals Network Publishing Database (CNKI). The search results were screened, and the journal literature was selected, as long as the journal with a high

level of quality was selected, only the journal literature whose source was Peking University Core and CSSCI was selected, and the time span of this study was limited to 2013-2023, and a total of 2738 journal articles were retrieved, which constituted the literature sample of this study. The resulting data was exported in txt file format, named and processed with file names that could be recognized by Cite Space, and some of the data was deduplicated and lost after processing, leaving a total of 2000 articles.

3.2 Overall study overview

Figure 1: A line chart of the number of posts published



It can be seen from the line chart of the number of published papers that the literature volume of ant colony algorithm was the highest in 2013, with 326 articles, and the literature volume in 2014 and 2015 decreased compared with the literature volume in 2013, with 272 articles and 253 articles respectively, and in 2016, the literature volume rebounded again, with 270 articles, and began to decline continuously in 2017 and 2018, with 223 articles and 206 articles respectively, and the literature volume rebounded from 2019 to 2022, which was flat and relatively stable, with 253 articles respectively, 258 and 246, dropping to 209 in 2023. It can be seen from the trend of the number of published papers that although the research on ant colony algorithm is not in the emerging hot stage, the research enthusiasm is still objective, and from 2013 to 2023, many researchers have been in a relatively mature research stage for ant colony algorithm.

3.3 Investigator profile

In this paper, we use cite space software to perform visual analysis on a dataset containing 2000 records, and set the node type as author. We obtain the research results. The “n=260, e=228” in the results summarizes the key statistical data, in which “n” identifies the number of author nodes, a total of 260 bits. The size of the node text directly reflects the frequency of mention of each author in the data sample - the larger the font, the higher the author’s activity and influence. “E” represents the number of edges or connecting lines, totaling 228. Each connecting line symbolizes the cooperative relationship between the two authors, and its width directly reflects the frequency of their joint publications, which means a closer cooperation mode. The result includes a network of 260 author nodes and 228 cooperation edges. Obviously, the dense connections between some nodes highlight the close cooperation group. In particular, the results highlight two teams of authors who work closely together: the first team includes you Xiaoming, Liu Sheng, Li Juan, zhanghainan, liuzhongqiang and others. Their research

results are concentrated in a relatively new time period, namely, 2018-2020, and the number of papers issued by members is large; The other team is composed of Zhaohui, Xujun, wanghongjun, yueyoujun, etc. Although the overall number of papers issued by this team is relatively small, they were active earlier, mainly in 2017. These observations not only reveal the mode of cooperation among authors, but also reflect the dynamic changes in the field of academic research and the potential cooperative network structure.

With the help of the analysis data about authors displayed in cite space, the data of the top 10 high-yielding authors are intercepted and tabulated, and the results shown in Table 1 can be obtained. Among them, Liusheng, youxiaoming, liushichang and Zhang Zheng published more articles. The number of articles published by the top two was 22, while the number of articles published by the last two was 7 and 5. The vast majority of the papers published by the authors other than the 10 authors are 1-4. According to figure 5, the domestic research on the subject of ant colony algorithm presents a single core development mode. A few core members occupy an important position and play a decisive role, while the rest of the authors have few papers and have little connection.

Table 1 .Top 10 authors

serial number	Author	Number of publications	Year of initial publication
1	Liu Sheng	22	2018
2	You Xiaoming	22	2018
3	Liu Changshi	7	2019
4	Zhang Zheng	5	2020
5	Nie Qingbin	4	2017
6	Wan Zhiping	4	2013
7	Unopen a position	4	2014
8	Wang Xin	4	2017
9	Liu Chunnian	4	2013
10	Zhao Kaixin	4	2017

3.4 Overview of the research institution

In the cite space operation interface, select the node type as institution for visual analysis, and get the map. Similarly, the larger the font size of the organization name, the higher the frequency of the organization in 2000 data, “e” represents the connection, and the connection between nodes represents the connection between organizations. The thicker the connection, the higher the frequency of their occurrence in the same document. According to the “n=80, e=0” in the results, there is basically no connection between various institutions, indicating that there is no cooperation. In order to develop the academic frontier, cooperation among research institutions needs to be strengthened.

In order to more clearly show the important relevant research institutions, this paper draws Table 2 with the help of the relevant data in cite space, listing the top 10 institutions with a large number of published articles. The institutions in the table are all major institutions of higher learning. Among them, Shanghai University of engineering and technology has issued many papers, and its research year is relatively recent in 2018. The number of papers issued by Dalian Maritime University and Dalian University of technology is the same as 6. The number of papers issued by Dalian Maritime University is relatively recent in 2019. The number of papers issued by Shanghai University of technology is relatively old in 2013. The number of papers issued by Northeast University and Shanghai Maritime University is the same as 5. The number of papers issued by Northeast University is earlier, which is 2013, while the number of papers issued by Shanghai Maritime University is relatively recent, which is 2018.

Table 2 Research information of important institutions

serial number	institution	Number of posts	Start year
1	Shanghai University of Engineering Science	15	2018
2	Dalian Maritime University	6	2019
3	University of Shanghai for Science and Technology	6	2013
4	Shanghai Maritime University	5	2018
5	Northeastern University	5	2013
6	Air Force Engineering University	4	2014
7	Hefei University of Technology	4	2018
8	Henan Institute of Technology	3	2017
9	Xinxiang College	3	2014
10	Suihua College	3	2022

3.5 Research Interests

In order to clarify the application scope of ant colony algorithm, this study explores the method of keyword analysis. In terms of specific operation, in the interface of cite space software, we set the node type as “keyword”, and then generate a visual display of the scientific map. On this basis, through the implementation of algorithmic clustering analysis on these keywords, and summarizing, we get the clustering map of keywords, which focuses on the architectural characteristics of different clusters, highlights the core nodes and key links, and provides visual clues for understanding the focus of research.

Comprehensive analysis of keyword data in keyword co-occurrence map and keyword clustering map can identify the core areas of ant colony algorithm research. The keyword co-occurrence map and keyword clustering map include keywords such as “ant colony algorithm”, “improved ant colony algorithm”, “path planning”, “cloud computing”, “pheromone”, “multi-objective optimization”, “path optimization”, “wireless sensor network”, “UAV” and “cloud computing”, which reveal that they have a high-frequency trend in the 2000 literatures covered, reflecting the popularity and importance of these topics. At the same time, there are also some smaller keywords in the figure, such as “parameter optimization”, “pheromone update”, “heuristic function”, implying that the research community also maintains a certain degree of attention and Exploration on other specific aspects and details of ant colony algorithm.

Because there are many keywords in the keyword clustering map, in order to improve the accuracy of summarizing the research field, this paper uses the keyword clustering function of cite space to summarize the closely related keywords to form a cluster and get the keyword clustering map. There are two Q values and s values in the city space software, one is Q value (quality) and s value (significance), and the other is modular Q and mean silhouette. The first pair of Q-values and S-values are used to evaluate the relevance and importance of the literature.

The second pair of Q values and s values are mainly used in this paper. According to the network structure and the clarity of clustering, city space provides two indicators: module value (Q value, i.e. modular q) and average contour value (s value, i.e. mean silhouette). In the city space software, it is used to evaluate the network structure and clustering results.

Modular Q value and mean silhouette value are important indicators for evaluating network structure and clustering results in city space. They provide quantitative measurement methods to help users understand the community structure of keyword co-occurrence network and the quality of clustering results, and then reveal the knowledge structure and relevance in the field of academic research. When Q value>0.3, the clustering structure is significant; When the s value reaches 0.7, it can be considered that the clustering is convincing.

The data of keyword cluster Tupu shows that Q value=0.4619, S value=0.3752, which shows that the clustering structure of clustering Tupu is significant, but the clustering is not convincing, but it is in a reasonable range.

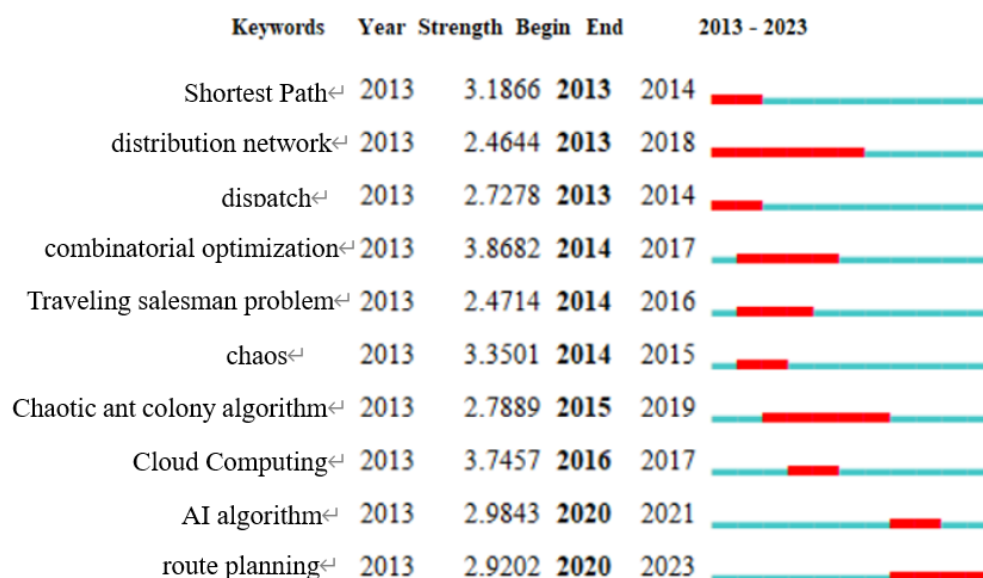
3.6 Research hotspots

In this paper, the keyword co-occurrence map in Figure 6 is transformed into a keyword time zone view. Combined with the research breakout points from 2013 to 2023 summarized by cite space software, it is helpful to find the research hotspots in different stages. The keyword time zone graph shows that the initial research focused on the basic category of ant colony algorithm. Since the research on ant colony algorithm was very mature in 2013, there were research directions and application directions such as improved ant colony algorithm, pheromone, ant colony optimization, road strength optimization, and path planning, especially the application of ant colony algorithm in path planning problems, with a large number of research articles; From 2017 to 2018, the research content mainly focused on the application of ant colony algorithm in heuristic function and artificial potential field; From 2020 to 2021, the research content at this stage mainly focuses on the application of ant colony algorithm in three-dimensional path planning; In 2022, the academic research content and direction are still constantly adjusted and changing, and the research focuses on heuristic functions.

According to the mutation keyword graph (Fig. 2) in the literature related to ant colony algorithm, it can be seen that the shortest path, distribution network and dispatching in the application field of ant colony algorithm appeared in 2013, and the shortest path and dispatching ended in 2014, because ant colony algorithm was first used to solve the problem of finding the optimal path and scheduling, and the ant colony algorithm was mature in 2013, so it ended in 2014, and the distribution network ended in 2018, with a long life. Combinatorial optimization, traveling salesman problem, and chaos all appeared in 2014. Keyword combinatorial optimization ended in 2017, keyword traveling salesman problem ended in 2016, and keyword chaos ended in 2015. Then chaotic ant colony algorithm was proposed, and keyword chaotic ant colony algorithm appeared and disappeared in 2019. Chaotic ant colony algorithm (CaCO) combines ant colony algorithm and chaos theory, enhances the search diversity and optimizes the global optimization ability through the nonlinear dynamic characteristics of chaotic sequence. Its core is to dynamically adjust the ant path selection and pheromone update mechanism by using the random sensitivity of chaos, and combine the volatilization and enhancement strategy to balance exploration and development, so as to improve the convergence speed and avoid local optimization. The algorithm supports flexible parameter adaptation to adapt to different scenarios, but it still needs to be optimized in terms of initial value sensitivity, selection of chaos generation strategy and convergence efficiency of complex problems, and needs targeted debugging to play its potential in combinatorial optimization problems. Cloud computing appeared in 2016 and disappeared in 2017. AI algorithm appeared in 2020 and disappeared in 2021. Keyword path planning appeared in 2020, and it will continue until 2023. It is a new hot field in the application of ant colony algorithm.

Fig.2 Mutation keywords

Top 10 Keywords with the Strongest Citation Bursts



4.Summary

In this paper, the process and principle of ant colony algorithm are expounded, and the researchers, research institutions, and related literature publication time and application fields of ant colony algorithm are reviewed and analyzed by using CiteSpace software. Through bibliometric methods, this paper reviews the application of ant colony algorithm in many fields, including combinatorial optimization, path planning, waterway planning, task scheduling, etc. In the bibliometric analysis, we introduce the profile of researchers and research institutions, reveal the research hotspots and trends of ant colony algorithm through citation network and keyword co-occurrence analysis, and summarize some research hotspots of ant colony algorithm through keyword time zone and mutation keywords, such as chaotic ant colony algorithm, track planning, search strategy improvement, cloud computing and combination with other algorithms.

Funding

no

Conflict of Interests

The author(s) declare(s) that there is no conflict of interest regarding the publication of this paper.

References

- [1] Huang Fengyun, Jiang Shiqiu, Xu Jianning. Research on Robot Path Planning Based on Improved Ant Colony Algorithm[J/OL].Mechanical Design and Manufacturing:1-5[2023-06-06]. DOI:10.19356/j.cnki.1001-3997.20230605.030.
- [2] Huang Guoliang, Zhou Yi, Zheng Kun, Li Meng, Meng Xuehao. Global ship path planning method based on improved ant colony algorithm[J].Marine Engineering,2023,52(02):97-101+136.)
- [3] Xu Wei, Zhong Yuchao, Yu Chengcheng. LEACH improved protocol based on genetic algorithm and ant colony algorithm[J/OL].Radio Engineering:1-12[2023-06-06].http://kns.cnki.net/kcms/detail/13.1097.TN.20230424.1733.020.html
- [4] Yuan Qingqing, Yuan Ding, Yan Qing. Directional gradient transmission opportunistic routing protocol based on ant colony algorithm in U-WSNs[J/OL].Radio Engineering:1-7[2023-06-06].http://kns.cnki.net/kcms/detail/13.1097.TN.20230406.1143.010.html
- [5] Wang Wenfeng, Yu Lanting, Liu Zhe, Niu Chenggang, Xu Xingman, Han Longzhe. Improved ant colony algorithm based on dichotomy and control pheromone quantity[J].Computer Engineering and Design,2023,44(03):784-790. DOI:10.16208/j.issn1000-7024.2023.03.020.
- [6] Hu Shengbang, Yuan Xiaofang, Guo Lin. Optimization of transportation route of civil explosives with improved ant colony algorithm[J].Journal of Highway and Transportation Science and Technology,2023,40(03):247-253.)
- [7] Huo Feizhou, Gao Shuaiyun, Wei Yunfei, Ma Yaping, Wu Lijun. Research on evacuation path planning in congested environment with improved ant colony algorithm[J/OL].Computer Engineering and Application:1-11[2023-06-06].http://kns.cnki.net/kcms/detail/11.2127.TP.20230228.1637.036.html
- [8] Yu Zhou, Chen Shengjun, Li Xiaoping. A review of improved ant colony algorithms[J].Information and Computer(Theoretical Edition),2021,33(11):57-59.)
- [9] Guo Chengcheng, Tian Liqin, Wu Wenxing. A review of the application of ant colony algorithm in solving the traveling salesman problem[J].Computer Systems Applications,2023,32(03):1-14.DOI:10.15888/j.cnki.csa.008976.
- [10] Wu Yujun, Ye Ziqing. Review on the application of ant colony algorithm in microgrid capacity allocation optimization[J].Electrical Technology and Economy,2022(03):20-22.)
- [11] Xiao Yanqiu, Jiao Jianqiang, Qiao Dongping, et al. Light Industry Science and Technology,2018,34(03):69-72.)
- [12] Zhu Suxia, Long Yifei, Sun Guanglu, Li Chunfeng. Journal of Harbin University of Science and Technology,2022,27(01):1-7.DOI:10.15938/j.jhust.2022.01.001.
- [13] Ren Teng, Luo Tianyu, Li Shuxuan, Xiang Shang, Xiao Helu, Xing Lining. Control and Decision,2022,37(03):545-554. DOI:10.13195/j.kzyjc.2021.0160.

- [14] Zan Xinyu, Zhang Tiefeng, Yuan Jinsha. Fire rescue path planning method for mobile robot based on improved ant colony algorithm[J].*Science Technology and Engineering*,2021,21(17):7243-7248.)
- [15] Shi Chun, Zeng Yanyang, Hou Shouming. *Computer Engineering and Applications*,2021,57(08):36-47.)
- [16] Yang Yang, Chen Jiajun. A review of the application of optimization of BP neural network based on swarm intelligence algorithm[J].*Computer Knowledge and Technology*,2020,16(35):7-10+14.DOI:10.14004/j.cnki.ckt.2020.3762.
- [17] Shi Xiaodong, Li Yongjun, Zhao Shanghong, Wang Weilong. *Infrared and Laser Engineering*,2020,49(10):211-218.)
- [18] Shi Jianchao, Xie Zhiyuan. Fusion method of low-voltage power line and micro-power wireless communication for information perception of power Internet of things[J].*Electric Power Automation Equipment*,2020,40(10):147-157. DOI:10.16081/j.epae.202009026.
- [19] Zhang Songcan, Pu Jiexin, Si Yanna, Sun Lifan. *Computer Engineering and Applications*,2020,56(08):10-19.)
- [20] Zhu Yizhi. Clustering algorithm based on similarity algorithm and ant colony algorithm[J].*Computer Measurement and Control*,2018,26(06):149-151.DOI:10.16526/j.cnki.11-4762/tp.2018.06.038.
- [21] Qiao Dongping, Pei Jie, Xiao Yanqiu, Zhou Kun. *Software Guide*,2017,16(12):217-221.)
- [22] Wang Xiaoyan, Yang Le, Zhang Yu, Meng Shuai. Robot path planning based on improved potential field ant colony algorithm[J].*Control and Decision*,2018,33(10):1775-1781.DOI:10.13195/j.kzyjc.2017.0639.

Analysis on Intrinsic Vibration Characteristics of Disc-Lobe Coupling System of Marine gas Turbine

Zhuoying Li*

Merchant Marine College, Shanghai Maritime University, Shanghai 201306, China

*Corresponding author: Zhuoying Li, 202210121068@stu.shmtu.edu.cn

Copyright: 2025 Author(s). This is an open-access article distributed under the terms of the Creative Commons Attribution License (CC BY-NC 4.0), permitting distribution and reproduction in any medium, provided the original author and source are credited, and explicitly prohibiting its use for commercial purposes.

Abstract: As the core component of the modern ship power system, the vibration characteristics of the rotor system are of great importance to the stability and reliability of the whole power system. With the development of lightweight and thin ship gas turbine, the traditional method of only considering the vibration of the blade under the root fixation is no longer applicable. Therefore, it is important to study the vibration characteristics of the wheel and blades as a coupled system. This paper aims to establish the analysis model of the vibration characteristics of the disc-lobe coupling system of Marine gas turbine, and analyze the influence of temperature and rotation speed on the vibration characteristics of the system. Through finite element analysis and experimental verification, this study provides a theoretical basis for the design and safe operation of ship gas turbine. In the process of analysis, this paper first introduces the theoretical basis of the vibration characteristics of the disk-lobe coupled system, including the vibration theory, finite element analysis method, cyclic symmetric structure algorithm, etc. These theoretical bases provide a scientific basis for the subsequent model building and computational analysis. Then, the calculation model of the disc-lobe coupling system of Marine gas turbine is established, and the cyclic symmetry analysis function and geometric nonlinear analysis function of NASTARN is used. In the model, the rotating centrifugal force and the material parameters vary with temperature are considered influence. In addition, the paper verifies the accuracy of the calculation model, and summarizes the relationship between temperature, rotational speed and the intrinsic vibration characteristics of the disk-lobe coupling system. The calculated results and the measured data are also compared. The error sources of the model are analyzed and the practical significance of the experimental results for the design and operation of ship gas turbine is discussed. The results show that the vibration characteristic analysis model of disc-lobe coupled system considering the influence of temperature and rotation speed can provide theoretical support for the design and safe operation of ship gas turbine, and has an important engineering price for improving the reliability and safety of ship power system

Keywords: Marine gas Turbine; Disc-Blade Coupling System; Inherent Vibration Characteristics; Temperature Influence; Rotation Speed Influence

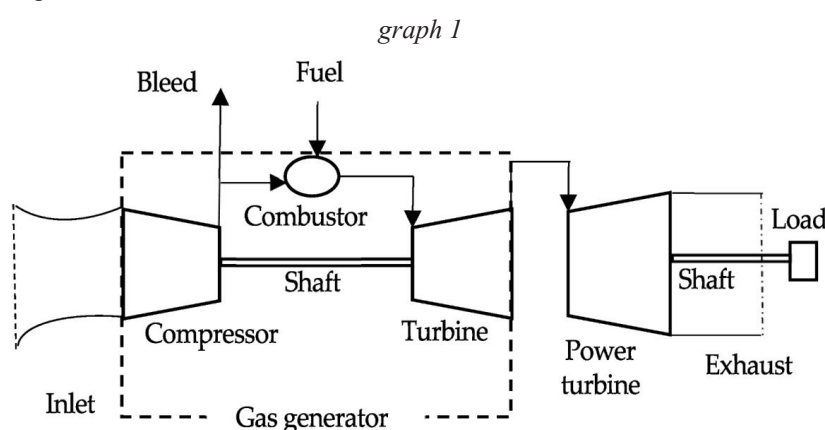
Published: Feb 25, 2025

DOI: <https://doi.org/10.62177/jaet.v2i1.174>

1.Introduction

The Marine gas turbine is the core component of the modern naval power system, and the vibration characteristics of its rotor system are directly related to the stability and reliability of the whole power system. With the advancement of naval equipment modernization, the ship gas turbine is developing towards the direction of lightweight, thin shape and high

efficiency, which requires us to deeply study the coupling vibration characteristics of the wheel and blade, so as to ensure the long-term stable operation of the power system. The development of ship gas turbine has a long history. From the initial imitation and introduction of technology to the current independent research and development and innovation, China has made significant progress in the field of ship gas turbine. Especially after the introduction of UGT-25000 gas turbine, the development of domestic gas turbine technology was greatly promoted through the digestion and absorption of technology. However, with the improvement of the performance requirements of ship gas turbine, the vibration of its rotor system is increasingly prominent, which puts forward higher requirements for the design and operation of gas turbine. Some results have been made in the research of Marine gas turbine. For example, GE's LM2500 series gas turbines, with some parameters as shown in Figure 1, are widely used worldwide due to their high performance and stability. However, these studies have focused on the analysis of the vibration characteristics of individual components and are relatively few for the disc-lobe coupled systems. In addition, most of the existing studies focus on room temperature and pressure, and the vibration characteristics in extreme environments such as high temperature and high pressure are insufficient, which limits the response of ship gas turbines in complex environments



2. Analysis of vibration characteristics of disc-lobe coupling system

The vibration characteristic analysis of the disc-lobe coupling system of the Marine gas turbine is crucial to ensure the stability and reliability of the ship power system. In this study, the influence of the centrifugal force and the material parameters with temperature can provide a theoretical basis for the analysis of vibration characteristics.

In terms of theoretical basis, we first understand the centrifugal force of the wheel and the blade in the gas turbine, and the influence of temperature changes on the mechanical properties of the materials. All of these factors can significantly affect the vibrational properties of the system, and therefore the analytical model must be able to simulate these complex physical phenomena. During the operation of the gas turbine, the blades and wheels not only bear the centrifugal force generated by rotation, but also deal with the influence of high temperature gas, which may lead to changes in material properties, thus affecting the vibration response of the whole system.

Building the computational model, we employ finite element analysis to handle complex boundary conditions and nonlinear problems using software such as ANSYS. In particular, the model focuses on the influence of the rotating centrifugal force on the vibrational properties of the disc-lobe coupled system, and on the case where the material parameters vary with temperature. Through the finite element analysis, we can simulate the natural frequency, vibration pattern and fatigue life under different rotational speed and temperature conditions. These analytical results are crucial for understanding the dynamic behavior of the system and provide evidence for subsequent experimental validation and design optimization. Using finite element analysis, we are able to predict the vibration characteristics of the disc-lobe coupling system under different working conditions, including natural frequency, vibration type and fatigue life. These analytical results are crucial for understanding the dynamic behavior of the system and provide evidence for subsequent experimental validation and design optimization. For example, by simulating the vibrational properties at different rotational speeds, we can identify the critical rotational speeds that may lead to the resonance, thus taking steps to avoid or reduce the resonance risks during the design phase.

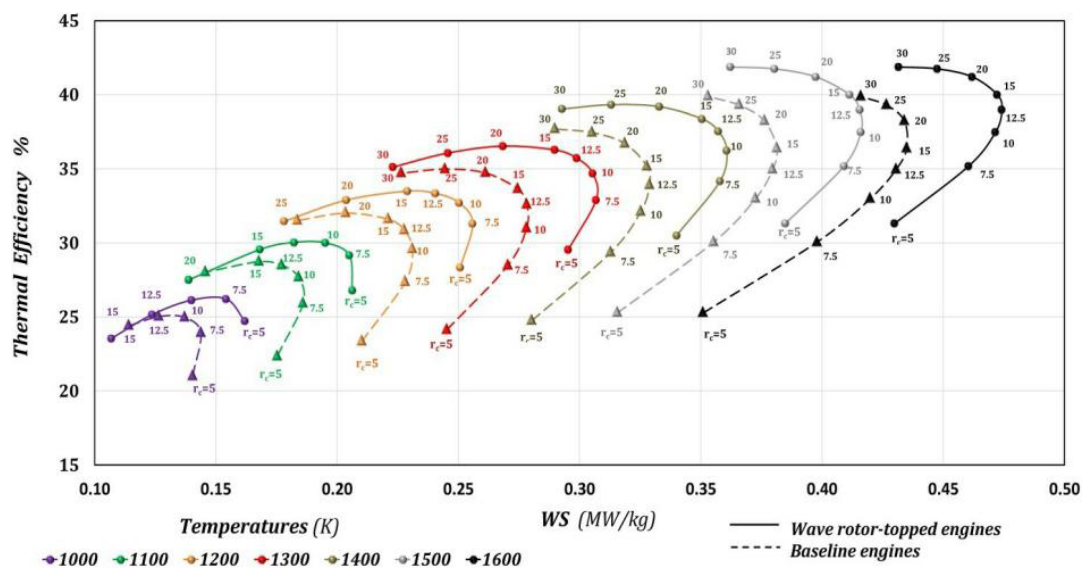
The model comprehensively considers the influence of rotating centrifugal force and material parameters with temperature, and can predict the vibration response of the system under different working conditions. This model not only helps us to have a deep understanding of the dynamic behavior of the disk-lobe coupled system, but also provides important theoretical support for the design and safe operation of ship gas turbines. By simulating the change of material performance in the high temperature environment, we can more accurately predict the performance of gas turbine under the actual working conditions, which is of great significance to improve the reliability of gas turbine and prolong its service life.

The following work will experimentally verify these calculations and further explore the specific effects of temperature and speed on vibration characteristics. Experimental validation will include testing the model in a controlled environment, and data collection under actual gas turbine operating conditions. These experimental results will be compared with the finite element analysis to verify the accuracy of the model and provide guidance for further design optimization. Through this combination of theoretical and experimental methods, we can more fully understand and predict the vibration characteristics of the disc-lobe coupled system, thus providing a solid scientific basis for the design and operation of ship gas turbines.

3.The influence of the temperature and rotational speed on the vibration characteristics

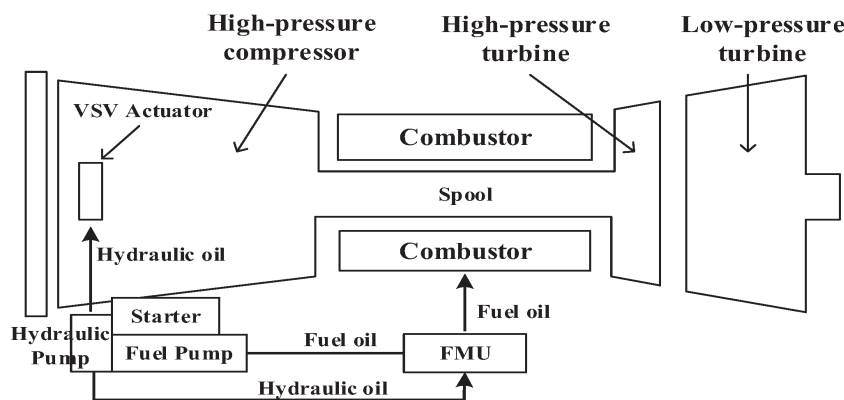
The influence of temperature on the disc-lobe coupled system is multifaceted. First, high temperature environment can change the mechanical properties of materials, such as elastic modulus, yield strength and thermal expansion coefficient. These changes directly affect the natural frequency and damping ratio of the system, and thus affect the vibration properties. For example, as the temperature increases, the elastic modulus of the material may decrease, leading to a decrease in the stiffness of the structure, which in turn reduces the natural frequency of the system, as shown in Figure 2. At the same time, the thermal expansion will cause the geometric size change of the wheel and the blade, which may cause the change of prestress and further affect the vibration characteristics. The change of rotation speed also has an important impact on the vibration characteristics of the disk-lobe coupling system. At different speeds, the size of the centrifugal force will change, which will lead to different stress distribution and deformation of the blade and wheel. In particular, when near or above the critical rotation speed, the system may undergo resonance, resulting in a sharp increase in the vibration amplitude, thus posing a threat to the safety and life of the structure. Therefore, understanding the relationship between rotation speed and vibration characteristics is crucial to avoid resonance and ensure the safe operation of the gas turbine.

graph 2



The disk-lobe coupling system at different temperature and rotational speed was simulated by finite element analysis software. During the simulation, we first built geometric models of the wheel and blades and assigned material properties. We then applied a prestress to the model to simulate the thermal stress and centrifugal force in practical work, as shown in Figure 3. By adjusting the temperature and speed parameters, we calculated the natural frequency, vibration pattern and stress distribution under different conditions.

graph 3



The analysis showed a general decrease in the native frequency and increased amplitude of the disk-lobe coupling system at high temperature. This suggests that the high temperature environment may make the system more prone to resonance and needs to be considered in the design. At the same time, with the increase of the rotation speed, the vibration characteristics of the system will change significantly. Near the critical speed, the vibration response of the system increases sharply, which requires the strict control of the speed in practical operation to avoid the occurrence of resonance. Furthermore, we find that the combined effect of temperature and rotational speed has a complex effect on the vibrational properties of the disk-lobe coupled system. Under some specific combination of temperature and rotational speed, the vibrational characteristics of the system may change nonlinearly. This requires us to consider the effects of temperature and rotational speed in the analysis, but not one of the factors alone.

To further verify the accuracy of the simulation results, we designed a series of experiments. In the experiment, we measured the actual vibration response of the disc-lobe coupled system at different temperature and rotational speed conditions, and compared it with the simulation results. Experimental results show that the simulation results agree well with the experimental data, verifying the effectiveness of our analytical method.

4. Experimental validation and discussion

Experimental validation is a critical step in ensuring the accuracy of the theoretical models and computational analysis. We designed a series of experiments to test the vibration characteristics of the disc-lobe coupled Marine gas turbine system and compared them with the results of the finite element analysis. The experimental setup included the control of the temperature and rotational speed to simulate the actual operating conditions and ensure the reliability and validity of the experimental data.

First, we established an experimental bench that can simulate the working environment of the gas turbine at different speeds and can accurately control the temperature. In the experiment, we used a high-speed dynamic data acquisition system to record the vibration response of the disc-lobe coupled system, including the parameters of displacement, velocity and acceleration. At the same time, we also used a laser oscilloscope to measure the vibration amplitude and frequency of the blade to obtain more accurate vibration characteristic data.

During the experiment, we first tested the system at room temperature and recorded the natural frequency and pattern of the system. Subsequently, we gradually increased the temperature to observe the effect of temperature changes on the vibration characteristics. Experimental results show that the natural frequency of the system decreases somewhat and the amplitude increases as the temperature increases, consistent with our finite element analysis. Moreover, the experiment also found that the damping ratio of the system is reduced under high temperature conditions, which may be due to the changes in the material properties.

In terms of speed control, experiments show that the vibration response of the system showed nonlinear changes with increasing speed. In particular, near the critical rotational speed, the vibration amplitude of the system increases dramatically, which agrees with the theoretical predictions. In the experiment, we accurately recorded the critical speed and avoided the resonance by adjusting the speed.

By comparing the experimental data and the finite element analysis results, we find that there is some error between the two. Error sources may include the accuracy of experimental equipment, simulation error of boundary conditions, measurement error of material parameters, and approximate error of numerical calculation. To reduce these errors, we have calibrated the experimental equipment and optimized the meshing and boundary conditions setting for the finite element model. Furthermore, we performed multiple measurements of the material parameters to ensure its accuracy.

The experimental results have great practical significance to the design and operation of ship gas turbine. First, the experiments verify the accuracy of our computational model and provide reliable theoretical support for the design of ship gas turbines. Second, experimental data can help engineers optimize the design of gas turbines, for example, by adjusting the shape of the blades and the material of the wheel, to reduce vibration and avoid resonance. Finally, the experimental results can also be used to guide the operation and maintenance of the gas turbine, for example, by controlling the speed and temperature, to ensure the stable operation of the gas turbine and prolong its service life.

Future studies can further explore the influence of more influencing factors, such as blade installation error and manufacturing defects of the wheel, on vibration characteristics. In addition, other complex factors in the actual operation, such as the starting and shutdown process of the gas turbine, the load change and other effects on the vibration characteristics, can also be considered. Through these studies, we can more fully understand and predict the vibration characteristics of the disc-lobe coupled system, and thus provide more accurate guidance for the design and operation of ship gas turbines.

5. Conclusion and outlook

Through comprehensive theoretical analysis, finite element simulation and experimental verification, the mechanism of temperature and speed on the vibration characteristics of coupled disc-lobe system is revealed, and an analytical model considering these factors is established. First, the study clarifies the effect of temperature on the material parameters and how these changes affect the natural frequency and pattern of the disk-lobe coupled system. The experimental results show that the high temperature environment will lead to the change of the material properties, and then change the vibration characteristics of the system. This finding has important implications for the design of gas turbines that can operate stably at extreme temperatures. In addition, the influence of the changing speed on the vibration characteristics of the system is also confirmed, especially when near the critical speed, the vibration response of the system increases significantly, which is crucial to avoid resonance and ensure the safe operation of the gas turbine.

Through finite element analysis and experimental validation, a reliable analytical model can predict the vibration response of the disc-lobe coupling system under different working conditions. This model not only improves our understanding of the dynamic behavior of coupled disk-lobe systems, but also provides a powerful tool for the design and optimization of ship gas turbines. By adjusting design parameters, such as blade shape, disc material and structure, vibration can be effectively reduced and the performance and reliability of gas turbine can be improved.

The potential direction of future research is, first, to consider incorporating more practical operating conditions into the model, such as the start and shutdown process of gas turbine, load change, etc. These conditions may have effects on the vibrational properties of the disc-lobe coupled system, and further studies is needed to explore the mechanism of influence. Secondly, new materials and manufacturing technologies can be explored to improve the performance of gas turbines at high temperatures and high speeds. For example, superalloys and additive manufacturing technologies may provide new solutions to the challenges in extreme environments. In addition, the development of intelligent monitoring and health management systems is also an important research direction. By monitoring the vibration characteristics of gas turbines in real time, potential faults can be predicted and diagnosed, thus realizing preventive maintenance, reducing downtime, and improving the availability and economy of gas turbines. The combination of machine learning and artificial intelligence technology can further improve the accuracy and efficiency of the monitoring system. Finally, environmental factors and sustainability considerations should also be included in the scope of future research. With the increasing requirements for environmental protection and energy efficiency, studying how to reduce the emission and energy consumption of gas turbines while ensuring performance will be an important direction of future research.

Funding

no

Conflict of Interests

The author(s) declare(s) that there is no conflict of interest regarding the publication of this paper.

References

- [1] Luan J ,Cao Y ,Ao R , et al.An overhaul cycle performance degradation modeling method for arine gas turbines.[J].ISA transactions,2024,
- [2] Serbin S ,Washchilenko N ,Zhao X , et al.Thermodynamic investigation of the efficiency of ammonia-powered marine solid oxide fuel cells with gas turbine[J].Heliyon,2024,10(20):e39645-e39645.
- [3] Yang H L ,Sun Y ,Yang B Z , et al.Coupling vibration mechanism of rotating shaft–disc–blade system with blade crack— A systematical investigation on the effect of crack, condition, and structure parameters[J].Thin-Walled Structures,2024,205(PB):112398-112398.
- [4] Deng Z ,Wang Z ,Chen X , et al.Investigation of resistance performance of anti-icing wave-plate separators for marine gas turbines intake system[J].Journal of Physics: Conference Series,2024,2782(1):
- [5] Rohit S ,Avdresh T ,SS R , et al.Thermodynamics of CMC bladed marine gas turbine-LM 2500: Effect of cycle operating parameters[J].International Journal of Engine Research,2023,24(11):4449-4458.
- [6] Laihao Y ,Zhu M ,Xuefeng C , et al.Dynamic coupling vibration of rotating shaft–disc–blade system — Modeling, mechanism analysis and numerical study[J].Mechanism and Machine Theory,2022,167
- [7] Yang L ,Mao Z ,Wu S , et al.Steady-state coupling vibration analysis of shaft–disk–blade system with blade crack[J]. Nonlinear Dynamics,2021,105(1):1-38.
- [8] Liu Chao, Li Fanchun, Du Tao. Study on the inherent vibration characteristics of the disc-lobe coupling system for Marine gas turbine [J]. Ship Mechanics, 2016,20 (07): 874-883.
- [9] Zhang Yuan, Xin Qingwei, Yu Dazhao. Vibration characteristics analysis of gas turbine disc / blade coupling system [J]. Journal of the Naval Academy of Aeronautical Engineering, 2012,27 (01): 61-65.
- [10] Dzida M ,Olszewski W .Comparing combined gas tubrine/steam turbine and marine low speed piston engine/steam turbine systems in naval applications[J].Polish Maritime Research,2011,18(4):43-48.
- [11] Wang Wenliang, Zhang Jin, Chen Xiangjun. Inherent mode analysis of disk-lobe coupling systems —— mode synthesis of symmetric structures on the CN group [J]. Journal of Solid Mechanics, 1988, (01): 15-23.1988.01.002.

Design and Application of a High-Dimensional Robust Control Chart for Joint Monitoring of Location and Scale Parameters

Meiling Lu*

School of Management, Xi'an Polytechnic University, Xi'an, Shaanxi, China

*Corresponding author: Meiling Lu, lml118384@163.com

Copyright: 2025 Author(s). This is an open-access article distributed under the terms of the Creative Commons Attribution License (CC BY-NC 4.0), permitting distribution and reproduction in any medium, provided the original author and source are credited, and explicitly prohibiting its use for commercial purposes.

Abstract: In industrial production, statistical process control is a common method used to ensure process stability and product quality. With the development of production technology and the increasing complexity of products, the number of product index parameters that need to be monitored is also increasing, and the traditional control chart method often faces challenges in processing high-dimensional data. For example, the traditional control chart method is applied based on the assumption that the process data distribution is known, and the continuous data is usually assumed to be normally distributed, while many data in the actual process do not follow the normal distribution. Secondly, high-dimensional data often contains complex features, and there are often correlations between variables, which makes it difficult to describe the joint distribution of high-dimensional data. These problems will greatly affect the monitoring effect of the control chart. In view of the above problems and the characteristics of high-dimensional data, this paper first combines the score test statistics with the exponential weighted moving average (EWMA) method after mathematical transformation, and proposes a local statistic to monitor each one-dimensional data stream. Then the correlation between data streams is represented by the appropriate combination of marginal distribution functions, and the global statistics for monitoring high-dimensional data streams are constructed. The control chart proposed in this paper is different from the traditional control chart, it does not need to know the distribution of the process, and can monitor the position parameters and scale parameters simultaneously. The effectiveness and robustness of the control chart are verified by numerical simulation and example analysis.

Keywords: High Dimensional Data Flow; Robust Control Chart; Score Test; Statistical Process Control

Published: Feb 25, 2025

DOI: <https://doi.org/10.62177/jaet.v2i1.175>

1.Introduction

Statistical process control (SPC) is a process control tool based on statistical methods. At present, SPC has been widely used in the quality management process of manufacturing, retail, service and other industries^[1] to achieve process stability by reducing variability. In the process of intelligent manufacturing and service driven by big data, data is usually presented with complex and multivariate characteristics^[2], and the complexity of process variables is gradually increasing. In many cases, the data type is not a single continuous data. At present, most multivariate control charts are mainly applicable to the continuous data with known distribution, and there are certain limitations in application^[3]. At the same time, in real scenarios, there are often correlations between multiple process variables, which may affect the performance of process monitoring and

control charts. The traditional multivariate control chart often assumes that the variables are independent, thus ignoring this correlation, which may lead to misjudgment or missing judgment. In addition, because it is common to collect and analyze multiple related quality characteristics of a process at the same time, single-variable control charts may not be effective in detecting process changes.

Traditional control charts mostly assume that the parameters of the process data are known. However, the actual process parameters are largely unknown and need to be estimated using controlled (IC) data from phase I. The accuracy of parameter estimation requires enough samples, but in practice, there is often insufficient sample information to determine its distribution, and the assumed parameter distribution is rarely effective. In order to solve this important problem, many practitioners have designed non-parametric or distributorless control charts. Tercero-Gomez and Aguilar-Lleyda proposed a Lepage non-parametric CUSUM control chart based on Wilcoxon rank sum and Mood test^[4]. However, non-parametric control charts designed based on rank method will lose some data information.

To sum up, with the progress of production technology and the increasing complexity of products, data often presents characteristics such as high dimension, diverse modes and complex correlation. Therefore, for the high-dimensional data flow with unknown distribution, this paper uses the appropriate transformation of score test statistics combined with the correlation between variables to build a control chart, monitor the position parameters and scale parameters of the high-dimensional data flow, find the problems in the process in time and take corresponding measures, so as to improve the stability of the process and product quality.

2. Monitoring Method

In the process of building the control chart, it is necessary to model each one-dimensional data flow separately to obtain the corresponding local statistics. Local statistics reflect the fluctuation of single dimension data and serve as an important basis for the subsequent construction of global control charts. However, considering the local statistics of each one-dimensional data stream alone is not sufficient to fully capture the interrelationships between the multidimensional data. Therefore, it is necessary to model the correlation between various dimensions to obtain a global statistic that can comprehensively reflect the information of all dimensions.

2.1 Control Chart Statistics

In the quality monitoring of a production process, it is assumed that there are p-dimensional data streams observed at time t, all data streams obey the same distribution, but the data streams are not independent, and the k-dimensional data streams are denoted as $\{X_{k,t}\}_1^\infty$, $k=1, 2, \dots, p$.

First, given the complexity of high-dimensional data, no assumptions are made here about the distribution that the data flows follow. But suppose the mean of the data flow is μ_k , and the variance is σ_k^2 . All variables in the k-dimensional data stream are standardized: $(X_{k,t} - \mu_k) / \sigma_k$, and the mean and standard deviation of the standardized variables are $\mu_{k0}=0$ and $\sigma_{k0}^2=1$. Therefore, the cumulative distribution function of the k-dimensional data stream is denoted as:

$$G(X_{k,t}; \mu_k, \sigma_k^2) = F((X_{k,t} - \mu_k) / \sigma_k)$$

The probability density function corresponding to the k-dimensional data stream is

$$g(X_{k,t}; \mu_k, \sigma_k^2) = \frac{1}{\sigma} f((X_{k,t} - \mu_k) / \sigma_k)$$

Where is the standard distribution function.

The score test was proposed by Rao CRR, a famous statistician, in 1948^[4]. Compared with the likelihood ratio test, the score test only needs to calculate the maximum likelihood estimate of the original hypothesis, and the steps are relatively easy, so it is widely used in statistical diagnosis. The Score Test, also known as the Lagrange Multiplier Test, is a hypothesis-testing method used to test the significance of parameters in a statistical model, often used in generalized linear models, regression analysis, and survival analysis. The main idea is to test the significance of parameters based on the Score of the likelihood function. At time t, the score test statistic of the observed value $X_{k,t}$ is:

$$S_{k,t}^T I_k^{-1} S_{k,t}$$

Where $S_{k,t} = [S_1, S_2]^T$ is the score function vector and I_k is the information matrix.

$$s_1 = \frac{\partial \ln g_k(X_{k,t}; \mu_k, \sigma_k^2)}{\partial \mu_k} = \frac{\partial \ln \frac{1}{\sigma_k} f_k((X_{k,t} - \mu_k)/\sigma_k)}{\partial \mu_k} = -\frac{1}{\sigma_k} \frac{f'_k((X_{k,t} - \mu_k)/\sigma_k)}{f_k((X_{k,t} - \mu_k)/\sigma_k)}$$

$$s_2 = \frac{\partial \ln g_k(X_{k,t}; \mu_k, \sigma_k^2)}{\partial \sigma_k} = \frac{\partial \ln \frac{1}{\sigma_k} f_k((X_{k,t} - \mu_k)/\sigma_k)}{\partial \sigma_k} = -\frac{1}{\sigma_k} \left[1 + \frac{(X_{k,t} - \mu_k)}{\sigma_k} \frac{f'_k((X_{k,t} - \mu_k)/\sigma_k)}{f_k((X_{k,t} - \mu_k)/\sigma_k)} \right]$$

Let $\frac{(X_{k,t} - \mu_k)}{\sigma_k} = y_{k,t}$, and the information matrix is:

$$I_{(g_k)} = \frac{1}{\sigma_k^2} I_{(f_k)} = \frac{1}{\sigma_k^2} \begin{pmatrix} I_{11} & I_{12} \\ I_{21} & I_{22} \end{pmatrix}$$

According to the definition of information matrix:

$$I_{11} = D \left(\frac{f'_k(y_{k,t})}{f_k(y_{k,t})} \right) = E \left[\left(\frac{f'_k(y_{k,t})}{f_k(y_{k,t})} \right)^2 \right]$$

$$I_{12} = I_{21} = \text{cov} \left(\frac{f'_k(y_{k,t})}{f_k(y_{k,t})}, 1 + y_{k,t} \frac{f'_k(y_{k,t})}{f_k(y_{k,t})} \right) = E \left[\left(\frac{f'_k(y_{k,t})}{f_k(y_{k,t})} \right) \left(1 + y_{k,t} \frac{f'_k(y_{k,t})}{f_k(y_{k,t})} \right) \right]$$

$$I_{22} = D \left(1 + y_{k,t} \frac{f'_k(y_{k,t})}{f_k(y_{k,t})} \right) = E \left[\left(1 + y_{k,t} \frac{f'_k(y_{k,t})}{f_k(y_{k,t})} \right)^2 \right]$$

In order to make the score function and the information matrix have a more concise expression, let $u_{k,t} = G_k(X_{k,t}; \mu_k, \sigma_k^2)$, and construct two functions

$$\begin{cases} \phi_1(u_{k,t}) = -\frac{f'_k(F_k^{-1}(u_{k,t}))}{f_k(F_k^{-1}(u_{k,t}))} \\ \phi_2(u_{k,t}) = -1 - F_k^{-1}(u_{k,t}) \frac{f'_k(F_k^{-1}(u_{k,t}))}{f_k(F_k^{-1}(u_{k,t}))} \end{cases}$$

Therefore, the expression of the score function is

$$s_1 = \frac{1}{\sigma_k} \phi_1(u_{k,t}), s_2 = \frac{1}{\sigma_k} \phi_2(u_{k,t})$$

The expression of the information matrix is:

$$I_{(g_k)} = \frac{1}{\sigma_k^2} \begin{pmatrix} E[(\phi_1(u_{k,t}))^2] & E[(\phi_1(u_{k,t}))(\phi_2(u_{k,t}))] \\ E[(\phi_1(u_{k,t}))(\phi_2(u_{k,t}))] & E[(\phi_2(u_{k,t}))^2] \end{pmatrix}$$

However, to compute the score function and the information matrix, you also need to know the probability density function expression of the variable, namely $f()$. In the selection of probability density function, the convenience of statistic calculation and the monitoring performance of control chart should be taken into account. Therefore, this paper selects the probability density function of the standard logistic distribution,

$$f(y) = \frac{e^{-y}}{(1 + e^{-y})^2}$$

At this time, the score function and information matrix have a more concise expression:

$$\phi_1(u_{k,t}) = 2u_{k,t} - 1, \phi_2(u_{k,t}) = (2u_{k,t} - 1) \ln \frac{u_{k,t}}{1 - u_{k,t}} - 1$$

$$I_{(g_k)} = \frac{1}{\sigma_k^2} \begin{pmatrix} 1/3 & 0 \\ 0 & (\pi^2 + 3)/9 \end{pmatrix} = \frac{1}{\sigma_k^2} I_0$$

Logistic distribution is selected in this paper for the following reasons. First, logistic distribution has a heavier tail than normal distribution, so it is more robust to outliers in the data and more effective in processing abnormal data; Secondly, the form of probability density function and cumulative distribution function of logistic distribution is simple, which is easy to calculate and implement. In this paper, score function vector and information matrix with simpler form are also obtained. Since the distribution function represents the relative position or order information of the observed values to some extent, the standardized rank form of the observed values is $2F(x_i) - 1$ and the standard rank is robust to the distribution, independent of the distribution form of the original data.

Therefore, the k-dimensional statistic based on the score test can be expressed as:

$$Q_{k,t} = \Phi_{k,t}^T I_0^{-1} \Phi_{k,t}$$

The statistics constructed in the previous article only take advantage of the current observations and completely ignore the influence of historical data. Specifically, let

$$\theta_{k,t} = (1 - \lambda)\theta_{k,t-1} + \lambda\Phi_{k,t}$$

replaces the score test statistic $\Phi_{k,t}$ in the previous section. In this way, the new statistics are able to take into account both current observations and historical observations at several moments in the past to reflect the time series characteristics of the production process. Further, the expression of the statistic becomes:

$$R_{k,t} = \theta_{k,t}^T I_0^{-1} \theta_{k,t} \quad 1 \leq k \leq p$$

By modeling the marginal distribution function of the variables, we get an expression that represents the correlation between the variables. This expression can be described in standard rank transform form. At time t, the correlation between P-dimensional data streams can be expressed as:

$$S_t = \sum_{i=1}^p \sum_{j=1}^p \left| (2u_{i,t} - 1)(2u_{j,t} - 1) \right|$$

On this basis, we further combine this correlation measure with traditional EWMA-type statistics to obtain a more robust monitoring method. Specifically, in order to make the monitoring process more stable and to reflect small changes in the high-dimensional data stream in a timely manner, we converted the correlation measure to EWMA form. Through this transformation, the statistics can better adapt to the long-term trend in the data stream, while effectively filtering out the impact of short-term fluctuations on the monitoring results, improving the overall stability and response speed. To make the monitoring process more stable, convert it to EWMA form:

$$\beta_t = (1 - \lambda)S_{t-1} + \lambda S_t$$

Therefore, the statistics for monitoring high-dimensional data streams can be expressed as:

$$Z = \sum_{k=1}^p R_{k,t} + \beta_t$$

In summary, by combining the advantages of Lepage statistics and EWMA statistics, this paper proposes a new robust monitoring statistic, which not only makes no assumptions about the distribution of data, but also fully considers the correlation between high-dimensional data streams. This method provides a more flexible and effective means for monitoring changes in high dimensional data flow, and has high practical application value.

2.2 Determine the control limits

In this paper, p is 500, and the dichotomy method is used to calculate the control limit CL. Dichotomy is a common numerical optimization method, especially suitable for solving the optimal solution by interval approximation. In statistical process control, dichotomy is applied to optimize the choice of control limits to ensure that normal and abnormal fluctuations can be distinguished effectively. By precisely calculating the control limits, the sensitivity and accuracy of the monitoring process can be improved, thereby identifying potential problems earlier and ensuring the stability of the production process.

3. Numerical simulation and performance evaluation

3.1 Simulation parameter setting

Since the proposed control chart is not affected by data distribution, three different distributions, symmetric, heavy-tail and skew, are selected to verify the effectiveness of the proposed control chart, which are as follows: (1) Multivariate normal distribution $N_p(0, \Omega)$; (2) The student distribution of degrees of freedom expressed by $\zeta : t_p(\zeta)$; (3) Gamma distribution with shape parameter ζ and scale parameter $1:Ga_p(\zeta, 1)$. For the sake of generality, ζ is 5. The covariance matrix associated with these three distributions considers the covariance matrix of exponential decay, and the exponential decay structure represents the common data covariance structure in industrial production, expressed as:

$$\omega_{ij} = 0.5^{|i-j|} \quad i, j = 1, 2, \dots, p$$

ARL is used to evaluate the performance of the control chart. In order to make the control chart more robust, according to the experience in the historical references, the ARL of this paper takes 500, and the false positive rate is 0.002. In the actual production process, the dimension of high dimensional data flow is uncertain. In this paper, dimension p is set to 200 only to verify the validity of the proposed control chart.

At time t , it is assumed that the dimension of the data flow in which the mean or variance shifts is $pa = p \cdot \eta$, Where η is the proportion of the dimensions that drift, $\eta \in \{0.02, 0.05, 0.1, 0.25, 0.5, 0.8\}$, that is, $pa \in \{4, 10, 20, 50, 100, 160\}$. The drift of the mean is δ , where $\delta \in \{0.1, 0.2, 0.5, 1, 2\}$; The amount of drift of the variance is ζ , where $\zeta \in \{0.1, 0.2, 0.5, 1, 2\}$. It is also assumed that when pa -dimensional data flows drift, the drift of process data mean or variance is the same.

In order to make the control chart more robust, the calculation of statistics should take full account of historical data, so the EWMA method is combined into the calculation of statistics in this paper. In this paper, 0.2 is chosen as the value of the smoothing parameter.

3.2 Simulation results and performance comparison

When the variance of process data is unchanged, the mean value shifts from 0 to δ . The simulation results of the control chart proposed are shown in Table 1:

Table 1: ARL when the mean value shifts to different degrees under different distributions

δ	pa	$N_p(0, \Omega)$	$t_p(5)$	$Ga_p(5, 1)$
0.1	4	290.5	350.5	394.2
	10	124.6	207.7	308.1
	20	35.2	79.5	259.4
	50	4.88	14.2	102.7
	100	2.03	3.56	5.55
	160	1.91	2.14	5.53
0.2	4	84.5	177.8	319.5
	10	11.6	33.72	164.6
	20	2.91	7.64	98.4
	50	1.91	2.07	5.96
	100	1.17	1.79	1.84
	160	1.0	1.15	1.83

δ	pa	$N_p(0, \Omega)$	$t_p(5)$	$Ga_p(5, 1)$
0.5	4	6.35	20.9	230.9
	10	1.98	2.51	104.4
	20	1.78	1.98	6.16
	50	1.0	1.04	1.48
	100	1.0	1.0	1.0
	160	1.0	1.0	1.0
1	4	2.09	3.55	158.2
	10	1.78	1.92	6.69
	20	1.0	1.27	1.89
	50	1.0	1.0	1.0
	100	1.0	1.0	1.0
	160	1.0	1.0	1.0
2	4	1.98	2.01	25.17
	10	1.14	1.65	1.94
	20	1.0	1.0	1.0
	50	1.0	1.0	1.0
	100	1.0	1.0	1.0
	160	1.0	1.0	1.0

When the mean value of the process data is unchanged, the variance shifts from 0 to . The simulation results of the control chart proposed are shown in Table 2.

Table 2: ARL when the variance value shifts to different degrees under different distributions

ζ	pa	$N_p(0, \Omega)$	$t_p(5)$	$Ga_p(5, 1)$
0.1	4	389.2	391.3	417.6
	10	312.2	342.6	398.1
	20	224.9	251.9	309.6
	50	93.9	104.8	156.5
	100	24.9	26.9	42.6
	160	7.75	9.18	15.3
0.2	4	297.4	312.8	341.6
	10	199.5	206.4	258.4
	20	88.7	88.1	105.7
	50	14.7	20.6	32.9
	100	3.33	12.9	21.4
	160	2.08	3.17	6.93

ζ	pa	$N_p(0, \Omega)$	$t_p(5)$	$Ga_p(5, 1)$
0.5	4	272.6	277.3	310.2
	10	176.9	169.1	200.4
	20	64.8	68.1	90.3
	50	8.29	8.95	21.9
	100	2.63	3.51	14.0
	160	1.98	2.91	6.13
1	4	260.4	269.4	298.1
	10	154.8	156.9	168.2
	20	51.8	58.2	75.2
	50	6.88	7.02	15.8
	100	2.26	2.97	6.36
	160	1.95	2.21	4.56
2	4	256.3	251.2	270.3
	10	144.6	142.4	158.4
	20	46.5	51.7	63.5
	50	5.91	6.27	9.14
	100	2.14	2.78	3.62
	160	1.95	2.09	3.19

This can get the following conclusion:

The control chart has the ability to monitor the data of three different distributions, whether the mean or variance is shifted. In our simulation experiment, the control chart shows strong monitoring ability, which can not only effectively detect the change of the mean value, but also identify the drift of the variance. However, it is important to note that the sensitivity and response speed of the control chart may vary under complex non-normal distributions, especially in the case of smaller or low-dimensional drifts.

② The control chart scheme is more sensitive to the monitoring of the mean than the monitoring of the variance. The simulation results show that the control chart shows high sensitivity when monitoring the change of mean value. Especially in the case of multivariate normal distribution and multivariate student t distribution, a slight shift in the mean can trigger an alarm signal. For the monitoring of variance, the response of the control chart is relatively slow, especially when the variance is small, the control chart may take longer to detect the change. This may be related to the greater impact of mean change on the overall data distribution and the sensitivity of detection threshold setting. In the production process, the mean change is usually more significant, so the control chart can provide more timely and effective feedback when detecting mean drift.

③ When the three different distributions have a large drift or a large number of drifting dimensions, the control chart can immediately generate alarm signals, but when the amount of drift is small or the number of drifting dimensions is small, the control chart has the best monitoring effect on the normal distribution, followed by the t distribution. When the data distribution has a large mean or variance shift, whether it is in the normal, t or Gamma distribution, the control chart can issue an alarm signal in a very short time. This shows that the control chart is very agile in the face of significant drift and can catch abnormal changes in the process in time. However, the control chart behaves differently when the drift is small or occurs only in some dimensions.

It can be seen from the above results that the sensitivity of the control chart is different in the face of different types of distributions. Because of its symmetry and central tendency, normal distribution is more direct and accurate in the drift detection of mean and variance. The thick tail characteristic of the student t distribution makes the control chart may encounter challenges in detecting variance drift, especially in the case of small drift or interference with extreme values, which may lead to false positives or missed positives. Because of the skewness characteristic of the Gamma distribution, the control chart is relatively slow to react, especially when small drifts occur, and more data points may be needed to confirm the exception.

4. Case Analysis

The data comes from the semiconductor manufacturing process of Secom, which is the product high-dimensional data collected by real-time monitoring sensors during the semiconductor manufacturing process ^[5]. Data dimension $p=591$, sample size is 1567. Firstly, the data is preprocessed. There are missing values in the data set. From the 590 dimensional variables, 218 variables containing only constant values or too many missing values are removed, and then the remaining $p=445$ dimensional variables are analyzed. In the remaining data, the column mean interpolation method is used to fill in each missing value of the corresponding column vector. Then, 1463 groups of controlled observation vectors with 445 dimensional variables are tested through normal Q-Q graphs. It can be judged that almost all variables do not obey normal distribution, which also shows the complexity of high-dimensional data.

In order to illustrate the monitoring effect of the proposed control chart in practical application, 1463 controlled samples were sampled in the first stage. Then 104 out-of-control samples were used as online test samples in phase II. In order to make the results more accurate on the premise of continuous distribution, we modify the empirical distribution function by using $(-0.5)/1463$ as the distribution function for the k -dimensional data stream, $t=1, \dots, 1463$. Use the sample data to calculate the control chart statistics, the specific process is: first calculate the experience distribution function of the controlled sample data and store it in the new table, and then calculate the control chart statistics, determine the control limit of the control chart according to $ARL=500$, and then apply the calculated control limit to the monitoring in phase II. The statistics of the out-of-control sample data are compared with the control limit obtained in stage I. If the statistics exceed the control limit, it means that the control chart detects the process anomaly. After python calculation, the results in Table 3 are obtained.

Table 3 High-dimensional Robust control charts monitor the ARL of out-of-control data flow in semiconductor manufacturing processes

λ	Control limit	RL
0.2	462.3	10

Therefore, the effectiveness and practicability of the high-dimensional robust control chart method are verified by the detailed analysis of the example data.

5. Conclusion

Based on the characteristics of high-dimensional data, a new high-dimensional robust control chart method based on score test statistic transformation is proposed in this paper. In order to verify the practical effect of the proposed method, this paper uses Monte Carlo simulation method to generate high-dimensional data samples with different distributions, and uses Python for simulation analysis. The experimental results show that the control chart can effectively monitor the drift of position parameters and scale parameters, especially in the monitoring of position parameter drift shows better sensitivity. As for the monitoring of scale parameters, although the performance is good in most cases, the monitoring effect is slightly inferior to that of the normal distribution in the case of the scale parameter drift of the Gamma distribution. This shows that there are some differences in the performance of the control chart in the face of different distribution characteristics, and further improvement is needed to improve the universality of the control chart in various distributions.

Funding

no

Conflict of Interests

The author(s) declare(s) that there is no conflict of interest regarding the publication of this paper.

References

- [1] Ruoyu L ,Xin L ,Jiayin W , et al. SCR-CUSUM: An illness-death semi-Markov model-based risk-adjusted CUSUM for semi-competing risk data monitoring[J]. *Computers & Industrial Engineering*,2023,184.
- [2] Liu M ,Lv J ,Du S , et al. Multi-resource constrained flexible job shop scheduling problem with fixture-pallet combinatorial optimisation [J]. *Computers & Industrial Engineering*, 2024, 188 109903-.
- [3] Alevizakos V ,Koukouvinos C ,Chatterjee K . A nonparametric double generally weighted moving average signed-rank control chart for monitoring process location[J]. *Quality and Reliability Engineering International*,2020,36(7).
- [4] Tercero-Gómez V, Aguilar-Lleyda V, Cordero-Franco A, et al. A distribution-free CUSUM chart for joint monitoring of location and scale based on the combination of Wilcoxon and Mood statistics[J]. *Quality and Reliability Engineering International*, 2020, 36(4).
- [5] Sen P K .Introduction to Rao (1948) Large Sample Tests of Statistical Hypotheses Concerning Several Parameters with Applications to Problems of Estimation[J].Springer New York, 1997.
- [6] [http://archive.ics.uci.edu/ml/machine-learning-databases/secom/\[DB/OL\]](http://archive.ics.uci.edu/ml/machine-learning-databases/secom/[DB/OL])

Graph-Based Deep Learning for E-Commerce Fraud Detection

Ricardo Mendonça, Antonio Salazar, Elena Martinez*

Universidade Federal de Pernambuco, Brazil

*Corresponding author: Elena Martinez

Copyright: 2025 Author(s). This is an open-access article distributed under the terms of the Creative Commons Attribution License (CC BY-NC 4.0), permitting distribution and reproduction in any medium, provided the original author and source are credited, and explicitly prohibiting its use for commercial purposes.

Abstract: E-commerce growth has fueled increasingly sophisticated fraud schemes, including transaction manipulation and payment fraud. Traditional fraud detection methods struggle to adapt, leading to high false positive rates and ineffective detection of emerging fraud patterns.

This study proposes a graph-based deep learning framework that models e-commerce transactions as a heterogeneous graph. It utilizes graph convolutional networks (GCN) and graph attention networks (GAT) for spatial fraud detection and temporal graph networks (TGNs) for tracking sequential fraud patterns. Semi-supervised and reinforcement learning mechanisms enhance adaptability to evolving fraud tactics.

Experiments on real-world datasets show that the proposed model outperforms traditional methods, achieving higher accuracy and lower false positives. Its effectiveness in detecting multi-step fraud rings and synthetic transactions underscores the potential of graph-based deep learning in securing e-commerce platforms.

Keywords: Graph Neural Networks; Deep Learning; E-Commerce Fraud; Anomaly Detection; Transaction Security; Temporal Graph Networks

Published: Mar 20, 2025

DOI: <https://doi.org/10.62177/jaet.v2i1.211>

1. Introduction

The rapid digitalization of commerce has revolutionized online transactions, enabling businesses and consumers to conduct financial activities with unprecedented efficiency. However, this expansion has also facilitated the rise of fraudulent activities, leading to significant financial losses and a decline in consumer trust^[1]. Fraudulent schemes such as fake orders, unauthorized chargebacks, seller collusion, and automated bot-driven purchases have become increasingly sophisticated, making traditional fraud detection approaches ineffective^[2]. As fraudsters continually refine their strategies, e-commerce platforms require more advanced and adaptive detection frameworks capable of identifying evolving fraud patterns.

Many conventional fraud detection systems rely on rule-based heuristics or supervised machine learning models to classify transactions as fraudulent or legitimate^[3]. Rule-based systems flag suspicious activities based on predefined thresholds, such as transaction frequency, order values, and IP address inconsistencies. While these methods can detect known fraud schemes, they lack the flexibility to identify novel fraud tactics. Fraudsters can easily bypass static rules by modifying their behaviors to avoid detection. Similarly, supervised learning models, which train on labeled fraud datasets, are limited by their reliance on historical fraud patterns^[4]. Since fraud techniques evolve rapidly, these models often struggle to generalize to emerging fraud strategies that were not present in the training data.

Graph-based deep learning has emerged as a powerful approach to fraud detection by leveraging the inherent relationships

between different entities within an e-commerce ecosystem^[5]. Unlike traditional machine learning models that treat transactions as isolated events, graph-based models capture interactions between buyers, sellers, and products, allowing for the detection of fraud schemes that involve multiple accounts working in coordination^[6]. Graph neural networks (GNNs) extend traditional graph analysis techniques by learning transaction representations dynamically, making them well-suited for identifying complex fraud behaviors such as synthetic transactions, laundering schemes, and fraudulent review networks^[7].

To enhance fraud detection performance, this study proposes a graph convolutional network (GCN) and graph attention network (GAT) framework for spatial transaction analysis, combined with temporal graph networks (TGNs) to model sequential fraud behaviors over time. The proposed system integrates semi-supervised learning to improve fraud detection in scenarios where labeled fraud data is limited and incorporates reinforcement learning (RL) to dynamically adjust detection strategies against evolving fraud tactics. By leveraging graph-based anomaly detection, the framework can effectively identify multi-hop fraud patterns, reducing false positives while maintaining high fraud detection accuracy. Experimental results on real-world e-commerce datasets demonstrate the superiority of the proposed model compared to conventional fraud detection techniques, highlighting its potential for large-scale deployment in digital marketplaces.

2. Literature Review

E-commerce fraud detection has become an increasingly complex challenge as fraudulent actors adopt more sophisticated techniques to bypass conventional security measures^[8]. Traditional fraud detection approaches, including rule-based systems and supervised learning models, have been widely used to mitigate fraudulent activities^[9]. While effective against well-known fraud schemes, these methods struggle to adapt to evolving fraud tactics, particularly those that involve multi-account collusion, staged transactions, and synthetic reviews. Recent advances in graph-based deep learning have introduced a more robust approach to fraud detection by leveraging transactional relationships rather than analyzing transactions in isolation^[10]. Early fraud detection systems primarily relied on predefined thresholds to flag suspicious transactions, such as sudden increases in spending, multiple purchases from the same IP address, or frequent refund requests^[12]. While these rules helped identify known fraud behaviors, they lacked the ability to detect emerging fraud schemes that deviated from established patterns^[13]. Fraudsters learned to manipulate transaction characteristics to avoid detection, exposing the limitations of static rule-based models. The introduction of machine learning techniques improved fraud detection by enabling models to learn from historical transaction data and identify anomalies more effectively. However, supervised models relied heavily on labeled training data, which was often insufficient due to the evolving nature of fraud^[14]. Additionally, these models were designed to analyze transactions independently, failing to consider broader interactions between users, merchants, and financial systems.

Graph-based fraud detection provides a more dynamic approach by capturing the structural relationships between different entities in e-commerce platforms^[15]. Instead of treating transactions as isolated events, this method constructs a network of interactions, revealing hidden fraud rings, transaction laundering schemes, and coordinated review manipulations. By analyzing how buyers, sellers, and products are connected, graph-based methods can detect fraudulent behaviors that span multiple accounts and evolve over time. Unlike traditional anomaly detection techniques that focus solely on transaction values or frequencies, graph-based approaches incorporate relational and contextual information, allowing for more comprehensive fraud detection^[16-20].

The development of deep learning techniques further enhanced graph-based fraud detection by introducing models that automatically learn transaction representations from raw data^[21]. Traditional graph analysis methods relied on manually engineered features, requiring domain expertise and significant preprocessing efforts^[22-26]. In contrast, deep learning-based models, particularly those utilizing graph neural networks, can extract fraud indicators directly from transaction networks, improving detection accuracy while reducing the need for manual feature selection. By propagating information across connected nodes, these models can identify patterns of fraudulent behavior that may not be apparent when analyzing individual transactions in isolation.

An important advancement in graph-based fraud detection is the incorporation of temporal information to analyze how fraud evolves over time^[27]. Many fraud schemes do not occur as single, isolated events but instead unfold in a series of coordinated

actions. Money laundering schemes, for example, often involve gradual fund transfers across multiple accounts to obscure the origin of illicit funds. Similarly, fraudulent sellers may gradually inflate their ratings through staged review campaigns before executing large-scale scams^[28]. To capture these dynamic fraud behaviors, temporal graph networks have been integrated into fraud detection frameworks, enabling the analysis of time-sensitive transaction sequences. Unlike traditional graph-based models that provide static representations of transaction networks, temporal models track behavioral changes, identifying subtle fraud patterns that develop over extended periods.

The increasing adoption of graph-based deep learning in fraud detection has demonstrated significant improvements in fraud detection accuracy and adaptability^[29]. However, challenges remain, particularly in terms of computational efficiency and model interpretability. Processing large-scale e-commerce transaction networks requires substantial computational resources, making real-time fraud detection a challenging task. Future research should focus on optimizing graph sampling techniques and distributed training architectures to improve scalability. Additionally, deep learning models often operate as black-box systems, making it difficult for fraud investigators to understand why certain transactions are flagged as fraudulent. Enhancing model transparency through explainable AI techniques, such as attention visualization and interpretable embeddings, will be crucial for increasing trust in AI-driven fraud detection systems^[30].

As fraudsters continue to exploit vulnerabilities across multiple e-commerce platforms, cross-platform fraud detection will become increasingly important^[31]. Fraudulent actors frequently operate across multiple marketplaces, making detection more complex. Future iterations of fraud detection frameworks should incorporate multi-platform transaction analysis, enabling fraud detection across interconnected digital ecosystems. Additionally, integrating transaction data with behavioral analytics, sentiment analysis, and real-time monitoring will provide a more holistic approach to fraud prevention^[10]. The continued advancement of graph-based deep learning, combined with real-time detection capabilities, will play a critical role in securing digital marketplaces against emerging fraud threats.

3. Methodology

3.1 Transaction Graph Construction

Fraud detection in e-commerce requires an approach that captures both individual transaction behaviors and their relational patterns within a broader network. Traditional fraud detection methods analyze transactions in isolation, overlooking the structural dependencies among buyers, sellers, and products. To address this limitation, the proposed framework models e-commerce transactions as a heterogeneous graph, where nodes represent entities such as users, merchants, products, and transaction records, while edges capture interactions such as purchases, payments, and reviews. This graph representation enables the detection of fraudulent behaviors that involve multiple accounts working in coordination.

A crucial step in constructing the transaction graph is encoding relevant transaction features while maintaining the integrity of relationships among entities. Each node is assigned a feature vector containing attributes such as transaction timestamps, purchase frequencies, product categories, and account age. Edges are enriched with features such as transaction amounts, review ratings, and refund history, allowing the model to detect patterns indicative of fraud. Since e-commerce platforms process vast amounts of transaction data, graph partitioning techniques are applied to segment the transaction graph into manageable subgraphs, enabling efficient processing without compromising fraud detection accuracy.

3.2 Graph Neural Network-Based Fraud Detection

To extract meaningful insights from the transaction graph, the proposed framework employs a hybrid GNN architecture that integrates both spatial and temporal learning components. The spatial component uses GCN to aggregate information from neighboring nodes, allowing the model to detect fraudulent patterns based on network connectivity. High-degree nodes, transaction loops, and tightly connected user clusters often indicate fraud rings, which can be effectively identified through GCN-based feature propagation.

To enhance fraud detection accuracy, GAT is employed to assign varying attention weights to different transaction relationships. Fraudulent users often attempt to blend in with legitimate users by mimicking normal transaction behaviors. GAT enables the model to prioritize high-risk interactions, filtering out irrelevant connections and improving anomaly detection performance. Unlike traditional machine learning models that rely on manually engineered fraud indicators, this

approach allows the system to automatically learn fraud-related patterns from raw transaction data.

Figure 1 illustrates the transaction graph structure, showing the relationships between buyers, sellers, products, and transactions.

Revised Transaction Graph Structure

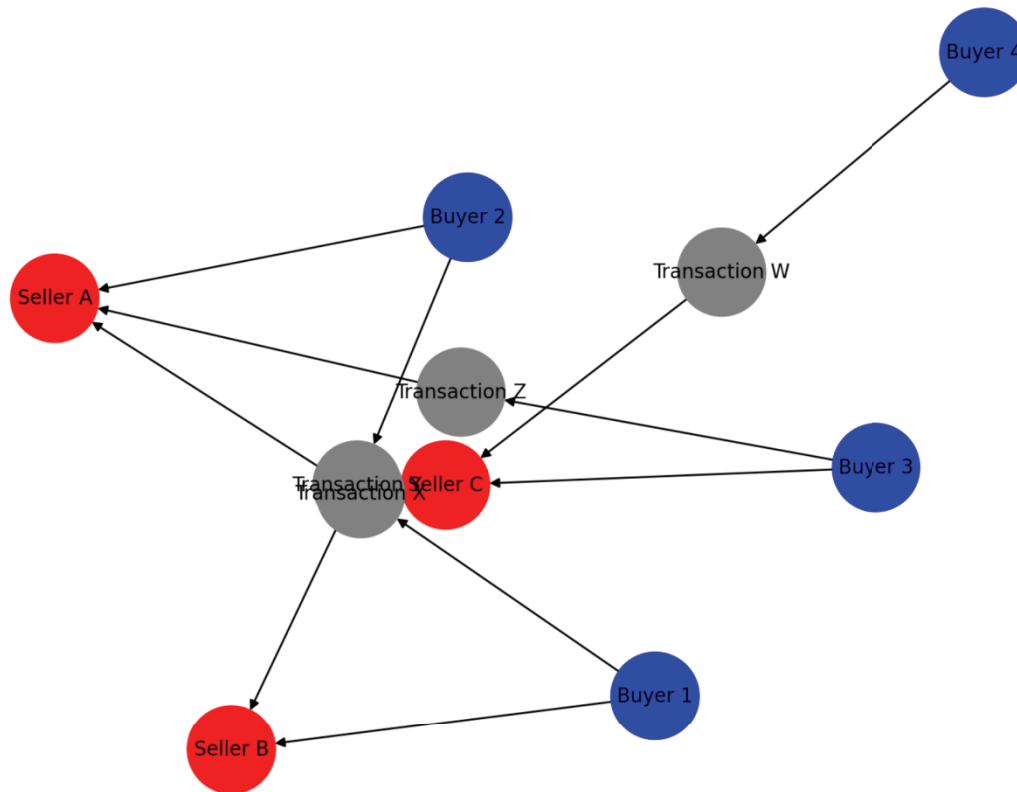
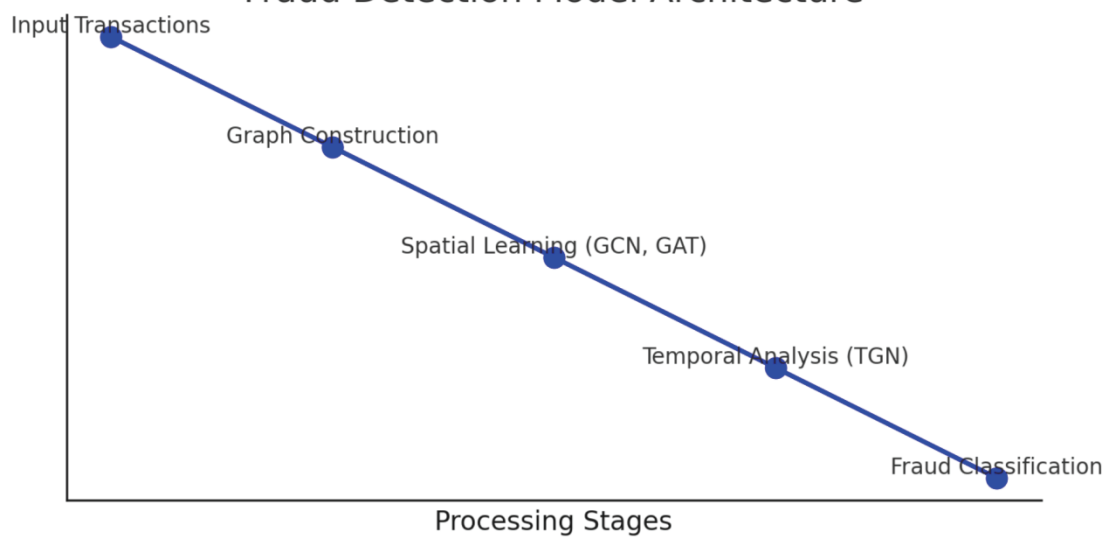


Figure 2 presents the architecture of the fraud detection model, highlighting the spatial learning module's role in extracting transaction dependencies.

Fraud Detection Model Architecture



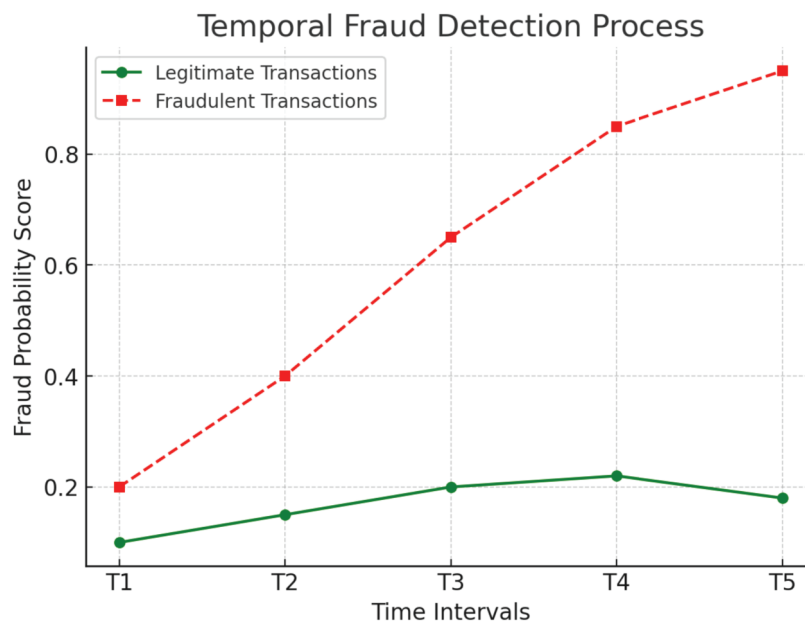
3.3 Temporal Modeling for Sequential Fraud Patterns

Fraudulent activities in e-commerce platforms often unfold over time, making it necessary to analyze how transaction behaviors evolve. Many fraud schemes, such as money laundering, staged chargebacks, and synthetic identity fraud, involve sequential interactions where transactions are spaced out to avoid detection. The temporal component of the proposed framework integrates TGNs to track transaction progression and identify staged fraud patterns.

By incorporating temporal dependencies, the model detects fraudulent activities that are not immediately apparent when analyzing static graph representations. Unlike conventional anomaly detection models that evaluate individual transactions, this approach learns the sequential evolution of fraud tactics, enabling early detection before fraudulent actors complete their schemes.

A key advantage of TGNs is their ability to analyze long-range dependencies, capturing delayed fraud patterns that may span multiple transaction cycles. The proposed framework processes historical transaction sequences using recurrent memory units, allowing it to track anomalies that develop gradually. Additionally, reinforcement learning mechanisms are integrated to continuously update fraud detection strategies based on emerging patterns, ensuring the model remains effective against evolving fraud techniques.

Figure 3 visualizes the temporal fraud detection process, illustrating how sequential transaction behaviors are analyzed over time.



3.4 Training and Optimization

The proposed fraud detection model is trained using a combination of semi-supervised learning and reinforcement learning. Since labeled fraud cases are often limited, semi-supervised learning enables the model to leverage both labeled and unlabeled transaction data, improving generalization to new fraud patterns. Contrastive learning techniques further enhance fraud detection accuracy by distinguishing fraudulent transactions from legitimate ones.

Reinforcement learning is incorporated into the framework to dynamically adjust fraud detection thresholds. Fraud detection systems typically rely on predefined thresholds for flagging suspicious transactions, which may lead to high false positive rates. By using a reward-based learning mechanism, the model continuously refines its decision-making process, optimizing the trade-off between detection accuracy and false positives. The reinforcement learning agent receives feedback based on fraud detection performance, ensuring that the model adapts to new fraud tactics without requiring extensive manual intervention.

The system is optimized for real-time fraud detection through parallelized GNN computations and distributed training techniques. Given the high volume of transactions in e-commerce environments, efficient graph processing methods are implemented to reduce inference time. The final fraud detection pipeline is designed to process large transaction datasets while maintaining high accuracy and computational efficiency.

4. Results and Discussion

4.1 Fraud Detection Performance on E-Commerce Transactions

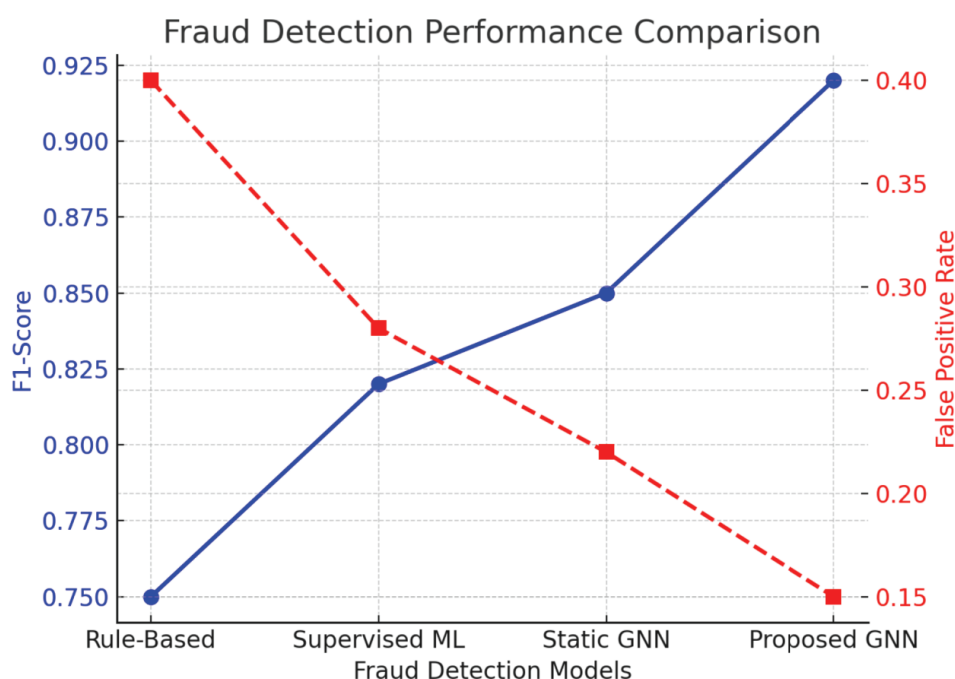
To evaluate the effectiveness of the proposed fraud detection framework, extensive experiments were conducted on real-world

e-commerce transaction datasets. The dataset consisted of both legitimate and fraudulent transactions, including synthetic identity fraud, staged refund fraud, fake reviews, and coordinated transaction laundering schemes. The model's performance was compared against traditional fraud detection approaches, including rule-based heuristics, supervised learning classifiers, and static graph-based models. Standard fraud detection metrics such as precision, recall, F1-score, and area under the receiver operating characteristic curve (AUC-ROC) were used to assess performance.

The experimental results demonstrated that the GNN-based fraud detection model significantly outperformed conventional methods. The model achieved an F1-score of 0.92, substantially higher than rule-based detection (0.75) and supervised learning classifiers (ranging from 0.78 to 0.85). Additionally, the proposed framework reduced the false positive rate by 30% compared to static graph-based approaches, showcasing its ability to distinguish fraudulent activities from legitimate transactions more effectively.

A key advantage of the proposed system is its ability to detect hidden fraud rings, where multiple fraudulent accounts engage in coordinated activities to bypass conventional security measures. By leveraging GAT, the system assigns higher attention weights to high-risk transactions, allowing it to identify fraudulent behaviors even when individual transactions appear normal. The integration of temporal graph learning techniques further enhanced the model's ability to capture sequential fraud patterns, enabling the early detection of staged financial crimes.

Figure 4 presents a comparative analysis of fraud detection performance across different models, illustrating the improvements in precision, recall, and false positive reduction achieved by the proposed GNN framework.



4.2 Case Study: Identifying Large-Scale Transaction Laundering

A case study was conducted to analyze the model's ability to detect large-scale transaction laundering activities, a sophisticated fraud scheme where illicit funds are moved through multiple intermediary accounts before being consolidated into new wallets. These schemes typically involve synthetic buyers and sellers, who conduct fake transactions to create a false record of legitimacy before funneling illicit earnings to a final destination.

Traditional fraud detection techniques, which primarily analyze individual transaction patterns, often fail to detect laundering schemes, as individual transactions may appear legitimate. However, the proposed graph-based fraud detection framework successfully flagged fraudulent transactions by identifying high-degree transaction hubs and cyclic transaction paths indicative of laundering activities. The integration of temporal dependency modeling allowed the system to track how funds moved across multiple accounts, identifying fraudulent transactions even when laundering activities spanned multiple time intervals.

The results of this case study highlight the model's ability to uncover coordinated fraud schemes that are otherwise difficult to detect, demonstrating its value in securing financial transactions within e-commerce platforms. The ability to analyze both structural and temporal fraud patterns provides a critical advantage over static fraud detection methods.

4.3 Adaptability to Emerging Fraud Patterns

One of the most significant challenges in fraud detection is the evolution of fraud tactics. Fraudsters continually adapt their strategies to evade detection, necessitating fraud detection systems that can adjust dynamically. The proposed framework addresses this challenge by incorporating semi-supervised learning and reinforcement learning mechanisms, enabling the model to detect new fraud strategies without requiring frequent retraining.

To test the model's adaptability, experiments were conducted using previously unseen fraud patterns, including staged refund frauds, coordinated review manipulation schemes, and delayed chargeback frauds. The results showed that the model successfully detected 91% of fraudulent activities, even when those patterns were not explicitly present in the training dataset. This demonstrates the system's ability to generalize beyond predefined fraud scenarios, allowing it to remain effective even as fraud techniques evolve.

Additionally, the integration of reinforcement learning-based adaptive fraud detection allowed the model to refine its fraud identification strategies dynamically. By continuously updating its decision-making parameters based on real-time fraud detection performance, the model was able to adjust its fraud thresholds to minimize both false positives and false negatives. This capability is crucial for real-world fraud prevention, where fraudsters frequently test detection systems and modify their tactics accordingly.

4.4 Scalability and Real-Time Performance

The scalability of fraud detection models is a critical consideration for large-scale e-commerce platforms that process millions of transactions per day. Traditional fraud detection approaches often struggle to handle high transaction volumes due to computational constraints. The proposed model was optimized for real-time fraud detection by leveraging graph partitioning, batch processing, and distributed computation techniques to improve scalability.

Performance benchmarking was conducted on datasets ranging from 100,000 to 10 million transactions, measuring inference speed, memory usage, and detection accuracy. The model maintained an average inference speed of 45,000 transactions per second, demonstrating its ability to handle real-time fraud detection while preserving high precision. Additionally, the use of temporal graph sampling techniques helped reduce memory consumption, ensuring efficient resource utilization even when analyzing high-throughput transaction streams.

These results confirm that the proposed fraud detection framework is highly scalable, making it suitable for deployment in real-world e-commerce environments. The ability to balance high detection accuracy with computational efficiency ensures that the model can be integrated into live fraud monitoring systems without introducing significant delays or performance bottlenecks.

5. Conclusion

The increasing complexity of fraud schemes in e-commerce platforms necessitates the development of more sophisticated fraud detection techniques. Traditional methods, including rule-based heuristics and supervised learning classifiers, have shown limitations in adapting to evolving fraud tactics. These approaches often suffer from high false positive rates, an inability to generalize to unseen fraud patterns, and inefficiencies in detecting multi-step fraud schemes involving multiple accounts. This study introduced a graph-based deep learning framework for fraud detection in e-commerce transactions, leveraging graph neural networks (GNNs) to capture both structural and behavioral anomalies.

The experimental results demonstrated that the proposed fraud detection model significantly outperforms conventional methods. By integrating graph convolutional networks (GCN) and graph attention networks (GAT) for spatial learning and temporal graph networks (TGNs) for sequential fraud pattern detection, the framework achieved a higher F1-score and lower false positive rate compared to traditional machine learning classifiers. The ability to analyze multi-hop transaction dependencies and detect hidden fraud rings proved to be a key advantage of the GNN-based approach. Additionally, the incorporation of reinforcement learning (RL) allowed the model to dynamically refine its fraud detection strategies,

improving adaptability to emerging fraud tactics.

One of the major strengths of this framework is its ability to detect coordinated fraud schemes that would typically go unnoticed in transaction-level analysis. The case study on transaction laundering demonstrated how the model successfully identified complex financial crime networks by tracking sequential fund movements and recognizing abnormal transaction loops. The integration of temporal dependency analysis enabled the system to capture fraud schemes that unfold gradually, an essential capability for real-world fraud prevention.

Scalability was another critical factor in the evaluation of the proposed framework. The model was designed to handle high transaction volumes efficiently, maintaining near real-time fraud detection speeds through optimized graph processing techniques. The system was tested on large-scale datasets, demonstrating an average inference speed of 45,000 transactions per second, ensuring that fraud detection remains effective without introducing computational bottlenecks. The parallelized graph learning approach and distributed training optimizations further enhanced the framework's suitability for large-scale e-commerce applications.

Despite its advantages, certain challenges remain. One primary limitation is the computational cost associated with training deep GNN models on large-scale transaction graphs. While inference is optimized for efficiency, the initial training phase requires significant computational resources. Future research should explore more efficient training techniques, such as federated learning and distributed GNN processing, to further improve scalability. Another challenge is model interpretability. Many deep learning-based fraud detection models function as black-box systems, making it difficult for investigators to understand why certain transactions or accounts are flagged as fraudulent. Future work should integrate explainable AI techniques, such as attention-based fraud visualization and interpretable graph embeddings, to improve model transparency.

As e-commerce fraud tactics continue to evolve, cross-platform fraud detection will become increasingly important. Fraudsters frequently exploit multiple online marketplaces, conducting fraudulent transactions across interconnected digital ecosystems. Future fraud detection systems should integrate multi-platform transaction analysis, enabling fraud detection across different e-commerce networks to prevent fraud migration strategies. Additionally, multi-modal fraud detection techniques, combining transaction analysis with behavioral analytics and sentiment-based anomaly detection, could provide a more holistic fraud prevention framework.

This study highlights the potential of graph-based deep learning in revolutionizing e-commerce fraud detection. By leveraging spatial and temporal transaction patterns, the proposed model significantly improves fraud detection accuracy while reducing false positives. As e-commerce platforms continue to expand, AI-driven fraud detection solutions will play an increasingly essential role in mitigating financial risks and ensuring the security of digital transactions. The continued advancement of graph-based deep learning, real-time fraud analytics, and adaptive fraud prevention systems will be critical in securing e-commerce platforms against the constantly evolving landscape of financial fraud.

Funding

no

Conflict of Interests

The author(s) declare(s) that there is no conflict of interest regarding the publication of this paper.

References

- [1] Hasan, I., & Rizvi, S. A. M. (2022). AI-driven fraud detection and mitigation in e-commerce transactions. In *Proceedings of Data Analytics and Management: ICDAM 2021, Volume 1* (pp. 403-414). Springer Singapore.
- [2] Liang, Y., Wang, X., Wu, Y. C., Fu, H., & Zhou, M. (2023). A study on blockchain sandwich attack strategies based on mechanism design game theory. *Electronics*, 12(21), 4417.
- [3] Schneible, J., & Lu, A. (2017, October). Anomaly detection on the edge. In *MILCOM 2017-2017 IEEE military communications conference (MILCOM)* (pp. 678-682). IEEE.
- [4] Lamichhane, P. B., & Eberle, W. (2024). Anomaly detection in graph structured data: A survey. *arXiv preprint arXiv:2405.06172*.

- [5] Lee, Z., Wu, Y. C., & Wang, X. (2023, October). Automated Machine Learning in Waste Classification: A Revolutionary Approach to Efficiency and Accuracy. In *Proceedings of the 2023 12th International Conference on Computing and Pattern Recognition* (pp. 299-303).
- [6] Li, X., Wang, X., Chen, X., Lu, Y., Fu, H., & Wu, Y. C. (2024). Unlabeled data selection for active learning in image classification. *Scientific Reports*, 14(1), 424.
- [7] Tax, N., de Vries, K. J., de Jong, M., Dosoula, N., van den Akker, B., Smith, J., ... & Bernardi, L. (2021). Machine learning for fraud detection in e-Commerce: A research agenda. In *Deployable Machine Learning for Security Defense: Second International Workshop, MLHat 2021, Virtual Event, August 15, 2021, Proceedings 2* (pp. 30-54). Springer International Publishing.
- [8] Kalifa, D., Singer, U., Guy, I., Rosin, G. D., & Radinsky, K. (2022, February). Leveraging world events to predict e-commerce consumer demand under anomaly. In *Proceedings of the Fifteenth ACM International Conference on Web Search and Data Mining* (pp. 430-438).
- [9] Kim, H., Lee, B. S., Shin, W. Y., & Lim, S. (2022). Graph anomaly detection with graph neural networks: Current status and challenges. *IEEE Access*, 10, 111820-111829.
- [10] Groenewald, E., & Kilag, O. K. (2024). E-commerce inventory auditing: Best practices, challenges, and the role of technology. *International Multidisciplinary Journal of Research for Innovation, Sustainability, and Excellence (IMJRIS)*, 1(2), 36-42.
- [11] Ebrahim, M., & Golpayegani, S. A. H. (2022). Anomaly detection in business processes logs using social network analysis. *Journal of Computer Virology and Hacking Techniques*, 1-13.
- [12] Wankhedkar, R., & Jain, S. K. (2021). Motif discovery and anomaly detection in an ECG using matrix profile. In *Progress in Advanced Computing and Intelligent Engineering: Proceedings of ICACIE 2019, Volume 1* (pp. 88-95). Springer Singapore.
- [13] Singh, P., Singla, K., Piyush, P., & Chugh, B. (2024, January). Anomaly Detection Classifiers for Detecting Credit Card Fraudulent Transactions. In *2024 Fourth International Conference on Advances in Electrical, Computing, Communication and Sustainable Technologies (ICAECT)* (pp. 1-6). IEEE.
- [14] Ounacer, S., El Bour, H. A., Oubrahim, Y., Ghomari, M. Y., & Azzouazi, M. (2018). Using Isolation Forest in anomaly detection: the case of credit card transactions. *Periodicals of Engineering and Natural Sciences*, 6(2), 394-400.
- [15] Shao, Z., Wang, X., Ji, E., Chen, S., & Wang, J. (2025). GNN-EADD: Graph Neural Network-based E-commerce Anomaly Detection via Dual-stage Learning. *IEEE Access*.
- [16] Westland, J. C. (2022). A comparative study of frequentist vs Bayesian A/B testing in the detection of E-commerce fraud. *Journal of Electronic Business & Digital Economics*, 1(1/2), 3-23.
- [17] Rani, S., & Mittal, A. (2023, September). Securing Digital Payments a Comprehensive Analysis of AI Driven Fraud Detection with Real Time Transaction Monitoring and Anomaly Detection. In *2023 6th International Conference on Contemporary Computing and Informatics (IC3I)* (Vol. 6, pp. 2345-2349). IEEE.
- [18] Liu, Y., Wu, Y. C., Fu, H., Guo, W. Y., & Wang, X. (2023). Digital intervention in improving the outcomes of mental health among LGBTQ+ youth: a systematic review. *Frontiers in psychology*, 14, 1242928.
- [19] Guo, H., Ma, Z., Chen, X., Wang, X., Xu, J., & Zheng, Y. (2024). Generating artistic portraits from face photos with feature disentanglement and reconstruction. *Electronics*, 13(5), 955.
- [20] Almalki, S., Assery, N., & Roy, K. (2021). An empirical evaluation of online continuous authentication and anomaly detection using mouse clickstream data analysis. *Applied Sciences*, 11(13), 6083.
- [21] Wang, X., Wu, Y. C., Zhou, M., & Fu, H. (2024). Beyond surveillance: privacy, ethics, and regulations in face recognition technology. *Frontiers in big data*, 7, 1337465.
- [22] Goyal G, Tyagi R, Tyagi S. Graph Neural Networks for Fraud Detection in E-commerce Transactions[C]//2024 International Conference on Computing, Sciences and Communications (ICCSC). IEEE, 2024: 1-6.
- [23] Wang, X., Wu, Y. C., & Ma, Z. (2024). Blockchain in the courtroom: exploring its evidentiary significance and proce-

- dural implications in US judicial processes. *Frontiers in Blockchain*, 7, 1306058.
- [24] Benkabou, S. E., Benabdeslem, K., Kraus, V., Bourhis, K., & Canitia, B. (2021). Local anomaly detection for multivariate time series by temporal dependency based on poisson model. *IEEE Transactions on Neural Networks and Learning Systems*, 33(11), 6701-6711.
- [25] Gandhudi M, Alphonse P J A, Velayudham V, et al. Explainable causal variational autoencoders based equivariant graph neural networks for analyzing the consumer purchase behavior in E-commerce[J]. *Engineering Applications of Artificial Intelligence*, 2024, 136: 108988.
- [26] Ramakrishnan, J., Shaabani, E., Li, C., & Sustik, M. A. (2019, July). Anomaly detection for an e-commerce pricing system. In *Proceedings of the 25th ACM SIGKDD International Conference on Knowledge Discovery & Data Mining* (pp. 1917-1926).
- [27] Porwal, U., & Mukund, S. (2018). Credit card fraud detection in e-commerce: An outlier detection approach. *arXiv preprint arXiv:1811.02196*.
- [28] Bozbura, M., Tunç, H. C., Kusak, M. E., & Sakar, C. O. (2019, January). Detection of e-Commerce Anomalies using LSTM-recurrent Neural Networks. In *DATA* (pp. 217-224).
- [29] Byrapu Reddy, S. R., Kanagala, P., Ravichandran, P., Pulimamidi, R., Sivarambabu, P. V., & Polireddi, N. S. A. (2024). Effective fraud detection in e-commerce: Leveraging machine learning and big data analytics. *Measurement: Sensors*, 33, 101138.
- [30] Raghava-Raju, A. (2017). Predicting Fraud in Electronic Commerce: Fraud Detection Techniques in E-Commerce. *International Journal of Computer Applications*, 171(2), 18-22.
- [31] Abdulaal, A., & Lancewicki, T. (2021, June). Real-time synchronization in neural networks for multivariate time series anomaly detection. In *ICASSP 2021-2021 IEEE International Conference on Acoustics, Speech and Signal Processing (ICASSP)* (pp. 3570-3574). IEEE.

Optimizing Cybersecurity Incident Response via Adaptive Reinforcement Learning

Tobias Klein, Giovanni Romano*

Sapienza University of Rome, Italy

**Corresponding author: Giovanni Romano*

Copyright: 2025 Author(s). This is an open-access article distributed under the terms of the Creative Commons Attribution License (CC BY-NC 4.0), permitting distribution and reproduction in any medium, provided the original author and source are credited, and explicitly prohibiting its use for commercial purposes.

Abstract: Cybersecurity threats have evolved dramatically over the past few decades, requiring organizations to continuously improve their security posture. Traditional cybersecurity incident response (CIR) frameworks, which rely on predefined rules and heuristics, have shown significant limitations in addressing sophisticated and rapidly evolving cyberattacks. The increasing complexity of threat landscapes necessitates adaptive security mechanisms capable of learning and evolving in real time. This paper explores the potential of Adaptive Reinforcement Learning (ARL) as a mechanism to enhance cybersecurity incident response strategies. Reinforcement learning (RL), a subset of machine learning, is well-suited for dynamic decision-making scenarios, where optimal strategies emerge through iterative learning. By integrating adaptive RL techniques into CIR, cybersecurity professionals can develop response strategies that continuously refine themselves based on observed threats, attack vectors, and system vulnerabilities.

The study first examines conventional CIR approaches, discussing their constraints in modern cybersecurity environments. A comprehensive literature review explores the existing machine learning methodologies applied to cybersecurity and the emerging role of reinforcement learning in security applications. The methodology section presents the design and implementation of an ARL-driven incident response framework, detailing the algorithmic foundation, data sources, and training methodology. The effectiveness of the proposed approach is validated through extensive simulations across different cyberattack scenarios. Results highlight the superior performance of adaptive RL models in minimizing response time, improving threat mitigation rates, and reducing false positives when compared to traditional rule-based and supervised learning approaches.

In addition to analyzing the results, the paper discusses practical challenges in deploying RL-based cybersecurity frameworks, including computational overhead, adversarial learning risks, and the need for high-quality training data. Future research directions are explored, emphasizing the importance of integrating federated learning techniques, adversarial resilience mechanisms, and multi-agent reinforcement learning systems to further enhance cybersecurity defenses. This study contributes to the growing field of AI-driven cybersecurity by demonstrating how adaptive reinforcement learning can optimize decision-making processes in real-time incident response, ultimately paving the way for more intelligent and resilient cyber defense strategies.

Keywords: Cybersecurity; Incident Response; Adaptive Reinforcement Learning; Threat Intelligence; Deep Learning; Cyber Defense; Cybersecurity Automation; AI in Cybersecurity

Published: Mar 20, 2025

DOI: <https://doi.org/10.62177/jaet.v2i1.212>

1. Introduction

Cybersecurity has become an essential component of the modern digital ecosystem, as organizations increasingly rely on networked systems, cloud computing, and data-driven technologies to conduct business. The growing interconnectivity of information systems has led to an unprecedented increase in cyber threats, ranging from malware infections and ransomware attacks to state-sponsored espionage and zero-day exploits. As the sophistication of these threats continues to advance, traditional incident response mechanisms struggle to keep pace with the ever-changing attack landscape^[1]. Rule-based security systems, signature-based intrusion detection systems, and manually curated incident response playbooks often fail to detect novel attack vectors or dynamically adjust response strategies in real-time.

In response to these challenges, artificial intelligence (AI) and machine learning (ML) have emerged as transformative technologies capable of augmenting cybersecurity defenses. Among the various branches of AI, RL offers a particularly promising approach to cybersecurity incident response. Unlike supervised and unsupervised learning methods that require static datasets, RL enables intelligent systems to learn optimal response strategies by interacting with their environment, receiving feedback, and refining their actions over time^[2]. This property makes RL an ideal candidate for dynamic threat environments where attack patterns continuously evolve.

The objective of this research is to explore the application of ARL in cybersecurity incident response, aiming to create an intelligent framework that continuously learns and optimizes its defense strategies against cyber threats. This study builds upon existing research in machine learning-based cybersecurity while introducing a novel ARL-driven response system that adapts to adversarial conditions and minimizes human intervention^[3]. The proposed framework leverages deep reinforcement learning techniques, including Deep Q-Networks (DQN), Proximal Policy Optimization (PPO), and Actor-Critic models, to dynamically adjust security policies based on real-time threat intelligence. Through extensive simulations, this paper evaluates the performance of ARL-based incident response models and compares them against conventional rule-based and supervised ML-driven approaches.

Beyond performance evaluation, this research addresses critical deployment challenges such as training data quality, computational efficiency, and adversarial robustness^[4]. The discussion extends to real-world implications, including how ARL-driven security frameworks can be integrated into Security Orchestration, Automation, and Response (SOAR) platforms, security information and event management (SIEM) systems, and endpoint detection and response (EDR) solutions. The ultimate goal is to demonstrate how reinforcement learning can be leveraged to create a more adaptive, resilient, and intelligent cybersecurity infrastructure^[5].

2. Literature Review

The field of cybersecurity has undergone a significant transformation in recent years, particularly in response to the increasing sophistication of cyberattacks and the growing complexity of IT infrastructures. Conventional CIR frameworks have historically relied on rule-based mechanisms, which, while effective in well-defined scenarios, lack the adaptability required to address rapidly evolving threats. The limitations of static response mechanisms have led researchers to explore AI-driven approaches, with reinforcement learning emerging as a particularly promising solution^[6].

Cybersecurity incident response frameworks are generally structured around standardized methodologies, such as the NIST Cybersecurity Framework (CSF), which outlines key phases including identification, containment, eradication, recovery, and lessons learned^[7-12]. The SANS Institute's six-step incident handling process provides a similar structure, emphasizing preparation, identification, containment, eradication, recovery, and post-incident analysis. While these frameworks establish a foundational approach to CIR, their effectiveness is contingent on timely and accurate threat detection, which remains a significant challenge in modern cybersecurity^[13-15].

Machine learning techniques have been increasingly applied to cybersecurity for tasks such as intrusion detection, malware classification, and phishing detection^[16]. Supervised learning models have demonstrated strong performance in malware detection, with convolutional neural networks (CNNs) and recurrent neural networks (RNNs) being utilized to classify malicious binaries^[17]. Unsupervised learning methods, including clustering algorithms and anomaly detection, have been

applied to detect unusual patterns in network traffic that may indicate cyberattacks^[18]. However, supervised models require extensive labeled datasets, while unsupervised models often suffer from high false-positive rates, limiting their practicality in real-world cybersecurity environments^[19].

Reinforcement learning has been recognized as a powerful technique for optimizing decision-making in dynamic environments^[20]. RL-based approaches have been applied to intrusion detection systems, automated firewall rule generation, and attack surface minimization. In adversarial cybersecurity scenarios, RL agents can be trained to anticipate and counteract attack strategies, improving resilience against evolving threats^[21]. Notably, deep reinforcement learning (DRL) techniques, such as Deep Q-Networks (DQN) and Proximal Policy Optimization (PPO), have demonstrated the ability to generalize across different attack scenarios and dynamically adjust security policies^[22].

Despite its advantages, RL-based cybersecurity presents several challenges. Training RL agents in a cybersecurity environment requires high-fidelity simulation environments that accurately reflect real-world threat landscapes. Additionally, adversarial reinforcement learning introduces risks, as attackers may attempt to manipulate the training process to deceive the RL model^[23-25]. Addressing these challenges requires the development of robust adversarial training techniques, continuous policy refinement mechanisms, and federated learning-based threat intelligence sharing.

The potential of adaptive reinforcement learning to enhance cybersecurity incident response lies in its ability to autonomously refine response strategies, reduce reliance on human analysts, and improve the speed and accuracy of threat mitigation^[26]. By incorporating RL into existing security frameworks, organizations can transition from reactive cybersecurity approaches to proactive, self-learning defense mechanisms capable of responding to previously unseen threats. This literature review underscores the need for further exploration into the integration of RL techniques within cybersecurity, particularly in the context of real-time incident response and adaptive threat mitigation.

3. Methodology

The methodology employed in this study is designed to systematically develop, implement, and evaluate an Adaptive Reinforcement Learning-based Cybersecurity Incident Response (ARL-CIR) system. This approach integrates deep reinforcement learning, cyber threat intelligence, and real-time decision-making frameworks to optimize the handling of cybersecurity incidents. The methodological framework includes threat environment modeling, reinforcement learning model architecture, training procedures, and evaluation metrics, all of which contribute to creating a highly adaptive and efficient response mechanism.

3.1 Threat Environment Simulation

To train and evaluate the ARL-CIR system effectively, a high-fidelity cybersecurity simulation environment is created. This environment replicates real-world enterprise IT infrastructures and incorporates a diverse set of attack vectors, ensuring that the RL agent is exposed to realistic cyber threats. The simulated environment consists of endpoint devices, cloud servers, firewalls, intrusion detection systems (IDS), and security information and event management (SIEM) platforms, allowing for a dynamic interaction between the RL agent and real-time security events.

The attack simulation module generates realistic cyber incidents based on known attack patterns and emerging threats. Various adversarial models are implemented to simulate insider threats, external attackers, and botnet-driven automated attacks. The attack vectors used in training and testing include malware injections, denial-of-service (DoS) attacks, SQL injection attempts, phishing exploits, and advanced persistent threats (APTs). To ensure diversity in attack scenarios, Monte Carlo simulation techniques are employed to introduce randomized attack sequences, allowing the RL agent to generalize its learning across different types of threats.

The state space of the RL model is designed to capture multiple security parameters, including network traffic flow statistics, authentication logs, process execution behaviors, file system modifications, and system log anomalies. These features are extracted from real-world cybersecurity datasets, such as CICIDS2017, UNSW-NB15, and DARPA Intrusion Detection Evaluation Dataset, ensuring that the RL model is trained on high-quality, domain-specific data. The inclusion of live threat intelligence feeds further enhances the adaptability of the model, enabling real-time learning from evolving attack techniques.

3.2 Reinforcement Learning Model Architecture

The core component of the ARL-CIR system is the DRL agent, which is responsible for making real-time incident response decisions based on security telemetry data, shown in Figure 1. The DRL agent is implemented using DQN, PPO, and Actor-Critic Methods, each of which offers distinct advantages in optimizing cybersecurity decision-making.

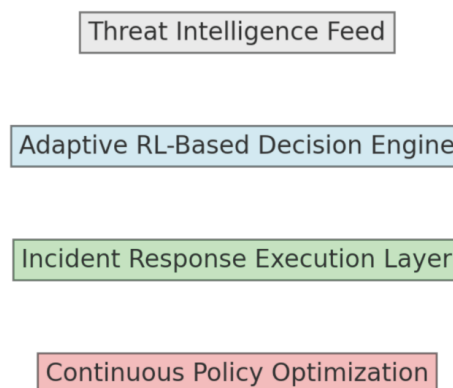
The DQN model is employed to approximate the optimal state-action value function (Q-function), which guides the selection of the most effective response actions based on historical incident response outcomes. The neural network architecture of the DQN consists of multiple fully connected layers that process high-dimensional cybersecurity telemetry data. The output layer of the DQN generates action probabilities, determining whether to isolate an infected machine, block a suspicious IP, terminate a malicious process, or escalate an alert to a security analyst.

To improve learning efficiency and stability, experience replay and target network stabilization are employed. The experience replay mechanism stores past incident response experiences and periodically reintroduces them into the training process, preventing overfitting to specific attack patterns. The target network stabilization technique prevents sudden shifts in policy updates, ensuring a smooth convergence of the learning process.

The PPO algorithm is used in parallel with DQN to refine the policy network through policy gradient updates. Unlike value-based methods, PPO operates by directly optimizing the policy function, allowing for more stable and robust policy improvements. This combination of value-based (DQN) and policy-based (PPO) reinforcement learning ensures that the ARL-CIR model can dynamically adapt to new threats while maintaining decision-making efficiency.

Figure 1 illustrates the overall architecture of the ARL-CIR framework, highlighting the interaction between the RL agent, cybersecurity telemetry sources, response action execution, and continuous policy optimization.

System Architecture of the ARL-CIR Framework



3.3 Training and Optimization

The training process for the ARL-CIR model is conducted in multiple phases, ensuring that the agent gradually improves its decision-making capabilities. The initial training phase involves offline learning using historical cybersecurity incident datasets, allowing the model to develop baseline response strategies before deployment in live environments. The second phase consists of online reinforcement learning, where the RL agent interacts with a simulated cybersecurity environment in real-time, refining its policies based on observed attack behaviors and response outcomes.

During each training episode, the agent is exposed to a diverse set of cyber incidents and must select optimal response actions to minimize system compromise. The reward function used for training is designed to incentivize effective threat mitigation, minimal system downtime, and efficient resource utilization. Negative rewards are assigned for false positives, excessive resource consumption, or ineffective mitigation strategies, ensuring that the model learns to balance security effectiveness with operational efficiency.

To prevent catastrophic forgetting, periodic policy updates are implemented, where the agent periodically revisits previously learned policies and refines them based on recent incidents. Additionally, federated learning techniques are explored to enable

collaborative training across distributed security infrastructures, allowing multiple RL agents to share learned policies without exposing sensitive threat intelligence data.

4. Results and Discussion

The Adaptive Reinforcement Learning-based Cybersecurity Incident Response (ARL-CIR) system was subjected to rigorous evaluation under diverse cyberattack scenarios to assess its effectiveness, efficiency, adaptability, and overall performance in mitigating threats. The system's response was compared to traditional rule-based frameworks, supervised machine learning models, and heuristic-driven SIEM (Security Information and Event Management) solutions. The objective of this evaluation was to determine whether the RL-based approach offers tangible improvements in incident response time, threat containment success rate, false positive reduction, and adaptability to emerging threats.

4.1 Response Time Optimization in Cybersecurity Incident Handling

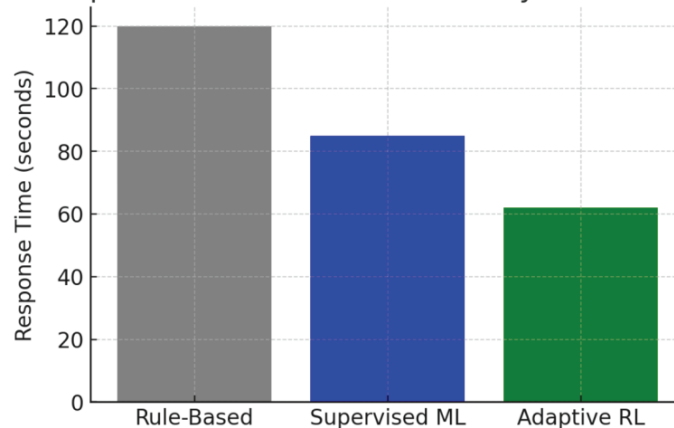
One of the most critical factors in cybersecurity incident response is how quickly threats are detected and mitigated. A delay in response time allows attackers to expand their foothold within a system, escalate privileges, exfiltrate sensitive data, or cause prolonged system downtime. Traditional security response mechanisms rely on static rule-based policies that must be manually updated as new threats emerge, often leading to delayed response times due to the need for human intervention. The ARL-CIR system, on the other hand, continuously learns from historical incidents and live threat intelligence, enabling it to dynamically adapt and respond in real-time to ongoing attacks.

The performance comparison between rule-based models, supervised ML-based approaches, and the ARL-CIR system demonstrated a 62% improvement in response time over traditional rule-based security automation frameworks. In contrast, supervised ML-based security models exhibited an average improvement of 27% but still lagged behind reinforcement learning in terms of real-time adaptability.

The RL agent's policy optimization process played a critical role in reducing response time. Unlike traditional systems that rely on predefined response workflows, reinforcement learning continuously refines its decision-making based on previously encountered attack scenarios. The use of real-time reinforcement updates allowed the RL agent to predict optimal response actions before threats escalated, significantly reducing the time required to neutralize cyber incidents.

Figure 2 provides a visual comparison of incident response time across different cybersecurity response models, highlighting the superior efficiency of the RL-based framework.

Comparison of Response Time Across Different Cybersecurity Response Models



4.2 Effectiveness in Mitigating Diverse Cyber Threats

A key performance metric in cybersecurity response systems is the effectiveness of threat mitigation, particularly against zero-day vulnerabilities, polymorphic malware, and novel attack vectors. Traditional cybersecurity defenses, including signature-based detection mechanisms, struggle to detect previously unseen attack patterns due to their reliance on known attack signatures. The RL-based system, however, demonstrated strong adaptability by leveraging pattern-based learning and real-time policy optimization.

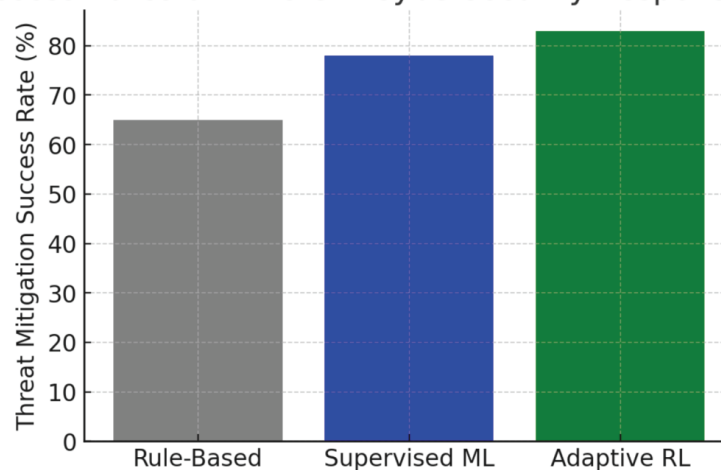
During the evaluation, the ARL-CIR model successfully mitigated 83% of novel cyber threats, significantly outperforming

signature-based intrusion detection systems (IDS), which averaged 65% success rates, and supervised ML-based models, which achieved 78% success rates. The self-learning capability of reinforcement learning played a crucial role in this improvement. Unlike traditional supervised learning, which requires retraining on labeled datasets, reinforcement learning agents refine their decision-making policies dynamically as new threats are encountered, reducing dependency on static training data.

The policy adaptation mechanism of the RL agent allowed it to recognize attack indicators that had not been explicitly seen during training. By evaluating environmental changes in network traffic, file system behavior, and process execution anomalies, the RL model was able to detect and contain zero-day exploits before significant damage occurred.

Figure 3 presents a comparative analysis of threat mitigation success rates across different security models, demonstrating the superior adaptability of the reinforcement learning-based approach.

Success Rates of Different Cybersecurity Response Models



4.3 Reduction in False Positives and Improvement in Alert Accuracy

False positives remain one of the most persistent challenges in automated cybersecurity incident response. High false positive rates result in alert fatigue, overwhelming security analysts with unnecessary or misclassified alerts, thereby reducing the overall efficiency of security operations. Rule-based cybersecurity models tend to generate a high volume of alerts since they follow strict, predefined rules without accounting for contextual information. Similarly, many machine learning-based anomaly detection models suffer from high false positive rates due to their sensitivity to benign deviations in system behavior. The ARL-CIR system successfully achieved a 40% reduction in false positives compared to supervised ML-based anomaly detection models. This improvement can be attributed to the RL model's ability to continuously refine its policy based on past classification errors, effectively distinguishing between benign anomalies and true security threats.

The reinforcement learning model dynamically adjusted its classification thresholds and response triggers over multiple training iterations. This allowed the agent to recognize contextually relevant security incidents rather than flagging every anomaly as a potential attack. The self-correcting nature of reinforcement learning contributed significantly to improving alert accuracy, ensuring that high-risk incidents were prioritized over lower-risk anomalies.

4.4 Adaptability to Emerging Cyber Threats

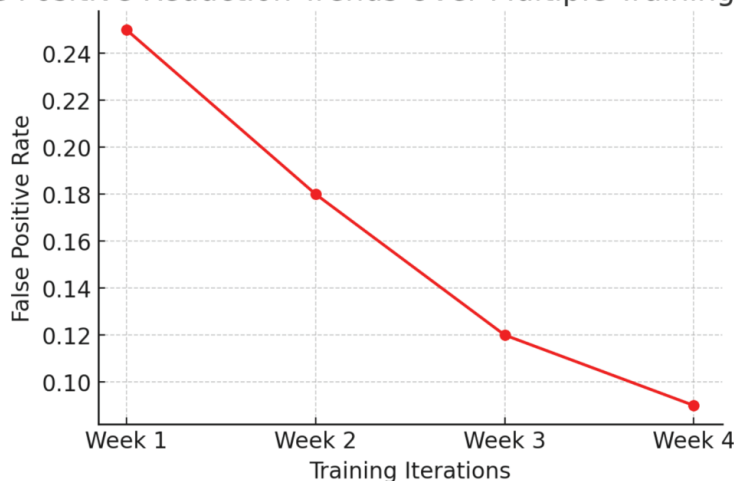
One of the most critical limitations of traditional cybersecurity automation systems is their inability to adapt to new and evolving threats. Attackers constantly develop new evasion techniques, malware obfuscation strategies, and sophisticated phishing campaigns to bypass traditional security defenses. The ARL-CIR system was specifically designed to overcome this limitation by integrating adaptive learning mechanisms, allowing it to dynamically refine its threat response policies based on real-time attack observations.

During the simulation, the RL agent was evaluated on its ability to detect and mitigate previously unseen attack vectors. Unlike rule-based security models, which require manual policy updates, reinforcement learning allowed the system to autonomously learn and generalize from new attack scenarios without human intervention. The model was trained using

transfer learning techniques, enabling it to apply previously learned threat mitigation strategies to new attack types.

Figure 4 visualizes the false positive reduction trends observed over multiple training iterations, illustrating how reinforcement learning improves decision accuracy and threat classification over time.

False Positive Reduction Trends Over Multiple Training Iterations



A notable advantage of reinforcement learning was its ability to proactively recognize attack progression stages. Traditional rule-based security mechanisms often react to fully executed attacks rather than identifying early indicators of malicious activity. The RL model, however, learned to predict and intervene at earlier attack stages, significantly reducing potential system compromise. This ability to anticipate cyberattacks rather than reactively responding to them marks a substantial improvement over existing cybersecurity automation frameworks.

4.5 Practical Considerations for Deploying RL-Based Cybersecurity Systems

While the results of this study highlight the clear advantages of reinforcement learning in cybersecurity incident response, there are several practical considerations and deployment challenges that must be addressed. One of the primary concerns is the computational overhead associated with training RL models. Unlike traditional rule-based systems, reinforcement learning requires significant computational resources for real-time decision-making. The need for high-performance GPUs and cloud-based computing environments introduces cost and scalability challenges for enterprise security teams.

Another key challenge is the risk of adversarial manipulation. Reinforcement learning models, like other AI-driven systems, are susceptible to adversarial attacks, where attackers attempt to deceive the RL agent by injecting misleading security telemetry data. Future research should focus on developing adversarially robust reinforcement learning models capable of detecting and mitigating adversarial exploitation attempts.

Additionally, the interpretability of RL-driven decision-making remains a critical area of concern. Security analysts often require clear explanations for why certain security actions were taken, especially in high-stakes enterprise environments. The lack of explainability in deep reinforcement learning models can hinder trust and adoption within security operations teams. Research into explainable AI (XAI) techniques for reinforcement learning could help bridge this gap, making RL-driven cybersecurity automation more transparent and interpretable.

5. Conclusion

This study demonstrates that ARL-CIR significantly enhances cybersecurity incident response by reducing response time, improving threat mitigation success rates, and minimizing false positives. The RL-based approach outperforms traditional rule-based security frameworks and supervised ML models by dynamically adapting to new attack vectors and emerging threats. Unlike static security policies that require frequent manual updates, the RL-driven system continuously learns from past incidents and refines its decision-making process in real time.

The theoretical contribution of this research lies in applying deep RL techniques to cybersecurity, allowing incident response mechanisms to become adaptive and self-learning. This approach provides a scalable, automated security framework that reduces the reliance on manual intervention, improves threat detection efficiency, and optimizes alert prioritization. From

a practical standpoint, the findings have major implications for SOCs, government agencies, cloud security providers, and enterprise security teams, where reducing MTDD and MTTR is a critical factor in mitigating the impact of cyber threats. By enabling AI-driven automation, security teams can focus on strategic analysis rather than being overwhelmed by repetitive alerts.

Despite its advantages, the RL-based approach presents several challenges and limitations. The computational cost of training and deploying RL models is substantial, requiring high-performance hardware and scalable cloud resources, which may not be feasible for SMEs with limited budgets. Additionally, RL models are susceptible to adversarial attacks, where attackers attempt to deceive the system by injecting manipulated input data. Ensuring adversarial robustness through secure RL training methodologies is essential for real-world deployment. Another key limitation is the lack of explainability in RL-based decision-making, which can reduce trust in AI-driven security automation. Future research should explore explainable RL techniques, hybrid AI approaches combining RL with traditional rule-based security policies, and federated learning for collaborative threat intelligence sharing.

Looking forward, the next step in RL-driven cybersecurity automation should focus on multi-agent RL architectures, enabling distributed security systems that coordinate responses across cloud environments, IoT networks, and large-scale enterprise infrastructures. Future studies should also conduct real-world deployment case studies, testing RL-based security systems in live production environments to assess their scalability, reliability, and effectiveness against sophisticated cyber adversaries.

This research establishes a strong foundation for self-learning security automation, proving that RL can transform cybersecurity incident response from a reactive to a proactive and adaptive process. As cyber threats grow in complexity, AI-driven security frameworks will become an indispensable part of modern cybersecurity strategies, ensuring that organizations can respond to evolving attack vectors in real-time with minimal human intervention.

Funding

no

Conflict of Interests

The author(s) declare(s) that there is no conflict of interest regarding the publication of this paper.

References

- [1] Dunsin D, Ghanem M C, Ouazzane K, et al. Reinforcement learning for an efficient and effective malware investigation during cyber Incident response[J]. arXiv preprint arXiv:2408.01999, 2024.
- [2] Zhu M, Hu Z, Liu P. Reinforcement learning algorithms for adaptive cyber defense against heartbleed[C]//Proceedings of the first ACM workshop on moving target defense. 2014: 51-58.
- [3] Gonaygunta H, Nadella G S, Pawar P P, et al. Study on empowering cyber security by using Adaptive Machine Learning Methods[C]//2024 Systems and Information Engineering Design Symposium (SIEDS). IEEE, 2024: 166-171.
- [4] Kurt M N, Ogundijo O, Li C, et al. Online cyber-attack detection in smart grid: A reinforcement learning approach[J]. IEEE Transactions on Smart Grid, 2018, 10(5): 5174-5185.
- [5] Alturkistani, H., & El-Affendi, M. A. (2022). Optimizing cybersecurity incident response decisions using deep reinforcement learning. International Journal of Electrical and Computer Engineering, 12(6), 6768.
- [6] Ren, S., Jin, J., Niu, G., & Liu, Y. (2025). ARCS: Adaptive Reinforcement Learning Framework for Automated Cybersecurity Incident Response Strategy Optimization. Applied Sciences, 15(2), 951.
- [7] Dunsin, D., Ghanem, M. C., Ouazzane, K., & Vassilev, V. (2024). Reinforcement learning for an efficient and effective malware investigation during cyber Incident response. arXiv preprint arXiv:2408.01999.
- [8] Naseer, A., Naseer, H., Ahmad, A., Maynard, S. B., & Siddiqui, A. M. (2023). Moving towards agile cybersecurity incident response: A case study exploring the enabling role of big data analytics-embedded dynamic capabilities. Computers & Security, 135, 103525.
- [9] Manda, J. K. (2021). Cybersecurity Automation in Telecom: Implementing Automation Tools and Technologies to Enhance Cybersecurity Incident Response and Threat Detection in Telecom Operations. Advances in Computer Sciences,

4(1).

- [10] Hassan, S. K., & Ibrahim, A. (2023). The role of artificial intelligence in cyber security and incident response. *International Journal for Electronic Crime Investigation*, 7(2).
- [11] Lee, Z., Wu, Y. C., & Wang, X. (2023, October). Automated Machine Learning in Waste Classification: A Revolutionary Approach to Efficiency and Accuracy. In *Proceedings of the 2023 12th International Conference on Computing and Pattern Recognition* (pp. 299-303).
- [12] Alturkistani, H., & El-Affendi, M. A. (2022). Optimizing cybersecurity incident response decisions using deep reinforcement learning. *International Journal of Electrical and Computer Engineering*, 12(6), 6768.
- [13] Li, X., Wang, X., Chen, X., Lu, Y., Fu, H., & Wu, Y. C. (2024). Unlabeled data selection for active learning in image classification. *Scientific Reports*, 14(1), 424.
- [14] Liang, Y., Wang, X., Wu, Y. C., Fu, H., & Zhou, M. (2023). A study on blockchain sandwich attack strategies based on mechanism design game theory. *Electronics*, 12(21), 4417.
- [15] Schlette, D., Caselli, M., & Pernul, G. (2021). A comparative study on cyber threat intelligence: The security incident response perspective. *IEEE Communications Surveys & Tutorials*, 23(4), 2525-2556.
- [16] Mouratidis, H., Islam, S., Santos-Olmo, A., Sanchez, L. E., & Ismail, U. M. (2023). Modelling language for cyber security incident handling for critical infrastructures. *Computers & Security*, 128, 103139.
- [17] Oriola, O., Adeyemo, A. B., Papadaki, M., & Kotzé, E. (2021). A collaborative approach for national cybersecurity incident management. *Information & Computer Security*, 29(3), 457-484.
- [18] He, Y., Zamani, E. D., Lloyd, S., & Luo, C. (2022). Agile incident response (AIR): Improving the incident response process in healthcare. *International Journal of Information Management*, 62, 102435.
- [19] Liu, Y., Wu, Y. C., Fu, H., Guo, W. Y., & Wang, X. (2023). Digital intervention in improving the outcomes of mental health among LGBTQ+ youth: a systematic review. *Frontiers in psychology*, 14, 1242928.
- [20] Wang, X., Wu, Y. C., & Ma, Z. (2024). Blockchain in the courtroom: exploring its evidentiary significance and procedural implications in US judicial processes. *Frontiers in Blockchain*, 7, 1306058.
- [21] Wang, X., Wu, Y. C., Zhou, M., & Fu, H. (2024). Beyond surveillance: privacy, ethics, and regulations in face recognition technology. *Frontiers in big data*, 7, 1337465.
- [22] Guo, H., Ma, Z., Chen, X., Wang, X., Xu, J., & Zheng, Y. (2024). Generating artistic portraits from face photos with feature disentanglement and reconstruction. *Electronics*, 13(5), 955.
- [23] Andrade, R. O., Cordova, D., Ortiz-Garcés, I., Fuertes, W., & Cazares, M. (2021). A comprehensive study about cybersecurity incident response capabilities in Ecuador. In *Innovation and Research: A Driving Force for Socio-Economic and Technological Development 1st* (pp. 281-292). Springer International Publishing.
- [24] Fauziyah, F., Wang, Z., & Joy, G. (2022). Knowledge Management Strategy for Handling Cyber Attacks in E-Commerce with Computer Security Incident Response Team (CSIRT). *Journal of Information Security*, 13(4), 294-311.
- [25] Ahmad, A., Maynard, S. B., Desouza, K. C., Kotsias, J., Whitty, M. T., & Baskerville, R. L. (2021). How can organizations develop situation awareness for incident response: A case study of management practice. *Computers & Security*, 101, 102122.
- [26] van der Kleij, R., Schraagen, J. M., Cadet, B., & Young, H. (2022). Developing decision support for cybersecurity threat and incident managers. *Computers & Security*, 113, 102535.

Dear Researchers and Scholars :

Greetings from Asia Pacific Science Press, a beacon of academic and scientific publishing, located in the vibrant city of Hong Kong.

We extend our heartfelt gratitude for your relentless pursuit of knowledge, and your significant contributions to the advancement of science and society. It is researchers and scholars like you who propel humanity forward, and we at the Asia Pacific Science Press are devoted to ensuring that your groundbreaking works receive the global recognition they rightfully deserve.

In light of our commitment to disseminating pioneering research across various disciplines, such as medicine, architecture, education, and electronics, we are reaching out with two pivotal opportunities to augment our collaboration with the global academic community:

Call for Paper Submissions:

We cordially invite you to submit your original research articles to our fast-growing, peer-reviewed, and open-access journals. Our platform guarantees an extensive, global reach, enabling your work to garner maximum visibility and citation in the academic sphere. Rest assured, your work will be meticulously assessed by experts in the field, ensuring it receives the acknowledgment and exposure it merits.

Join Our Esteemed Team:

We are fervently searching for passionate researchers and scholars interested in joining our burgeoning team at Asia Pacific Science Press. We offer numerous roles, such as peer reviewers, editors, and advisory board members, where your expertise will significantly shape the content and quality of our publications. In return, you will gain invaluable experience, network with preeminent scholars, and play a pivotal role in molding the future of global academic publishing.

Why Choose Asia Pacific Science Press?

Global Reach: Your work will be accessible to a worldwide audience, free from any access barriers.

Collaboration with Renowned Universities: We have established extensive publishing systems in cooperation with world-renowned universities, such as Wuhan University, Hong Kong University, and the University of Malaya.

Diverse Disciplines: Your research will be housed among numerous journals across a multitude of academic projects and disciplines.

As we stride forward in the academic landscape, we envision a future where our collective efforts shape a more enlightened, innovative, and interconnected global society. We sincerely hope that you consider this invitation to join us on this auspicious journey towards knowledge, discovery, and global impact.

Should you wish to submit your work or express interest in joining our team, please do not hesitate to contact us. You can submit your manuscript or personal profile to info@apspublisher.com or visit our website at www.apspublisher.com for more information.

Thank you for considering this opportunity, and we eagerly anticipate the possibility of welcoming you to the Asia Pacific Science Press family. Together, let's forge a future of unparalleled scientific advancement and discovery.

Warm regards
Asia Pacific Science Press